Published in final edited form as:
Neuropharmacology. 2009 February ; 56(2): 541–555. doi:10.1016/j.neuropharm.2008.10.012.

Modulation of GABAergic and glutamatergic transmission by ethanol in the developing neocortex: an *in vitro* test of the excessive inhibition hypothesis of Fetal Alcohol Spectrum Disorder

Jennifer L. Sanderson, **L. Donald Partridge**, and **C. Fernando Valenzuela**
Department of Neurosciences, University of New Mexico Health Sciences Center Albuquerque, NM 87131, U.S.A.

Summary

Exposure to ethanol during development triggers neuronal cell death and this is thought to play a central role in the pathophysiology of fetal alcohol spectrum disorder (FASD). Studies suggest that ethanol-induced neurodegeneration during the period of synaptogenesis results from widespread potentiation of $GABA_A$ receptors and inhibition of NMDA receptors throughout the brain, with neocortical layer II being particularly sensitive. Here, we tested whether ethanol modulates the function of these receptors during this developmental period using patch-clamp electrophysiological and Ca^{2+} imaging techniques in acute slices from postnatal day 7–9 rats. We focused on pyramidal neurons in layer II of the parietal cortex (with layer III as a control). Ethanol (70 mM) increased spontaneous action potential-dependent GABA release in layer II (but not layer III) neurons without affecting postsynaptic $GABA_A$ receptors. Protein and mRNA expression for both the Cl^- importer, NKCC1, and the Cl^- exporter KCC2, were detected in layer II/III neurons. Perforated-patch experiments demonstrated that E_{Cl}^- is shifted to the right of E_m; activation of $GABA_A$ receptors with muscimol depolarized E_m, decreased action potential firing, and minimally increased $[Ca^{2+}]_i$. However, the ethanol-induced increase of GABAergic transmission did not affect neuronal excitability. Ethanol had no effect on currents exogenously evoked by NMDA or AMPA receptor-mediated spontaneous excitatory postsynaptic currents. Acute application of ethanol in the absence of receptor antagonists minimally increased $[Ca^{2+}]_i$. These findings are inconsistent with the excessive inhibition model of ethanol-induced neurodegeneration, supporting the view that ethanol damages developing neurons via more complex mechanisms that vary among specific neuronal populations.

Keywords

neocortex; release; neurotransmitter; development; excitability; alcohol

Introduction

The complex structure of the human neocortex underlies increased behavioral and cognitive capacity that allows for enhanced sensory perception, motor control, spatial reasoning, and conscious thoughts (Bystron et al., 2008; Guillery, 2005; Markram et al., 2004; O'Leary et al., 2007). The neocortex is composed of six layers with functionally distinct subdivisions,

Corresponding Author: C. Fernando Valenzuela, M.D., Ph.D., Department of Neurosciences, MSC08 4740, 1 University of New Mexico, Albuquerque, NM 87131-0001, U.S.A., Phone (505) 272-3128, Fax (505) 272-8082, fvalenzuela@salud.unm.edu.

which contain diverse neuronal populations that make both local and extrinsic connections (O'Leary et al., 2007). These layers originate from a homogenous pseudo-stratified epithelium that lines the lateral ventricle in the dorsal telencephalon. Through a coordinated sequence of proliferation and migration, the layers form in an 'inside-out sequence' with the last migrating cells arriving at the most superficial portion of layer II by postnatal day (PD) 6 (Ignacio et al., 1995; O'Leary et al., 2007; Parnavelas, 2000). In rodents, cortical GABAergic interneurons arise from pseudo-stratified epithelia that lines the medial ganglionic eminence (Anderson et al., 2001; Parnavelas, 2000). After arriving in the neocortical layers, interneurons associate with radial glial and migrate to their final position in the neocortex. Alterations in neocortical development have been linked to a number of diseases including autism, epilepsy, schizophrenia, and fetal alcohol spectrum disorder (FASD) (Ben-Ari, 2006; Guerri, 1998; Levitt et al., 2004; Mattson et al., 1999). FASD, which results from ethanol (EtOH) exposure at different times during fetal development, results in a broad spectrum of abnormalities, including facial anomalies, growth retardation, and central nervous system (CNS) dysfunctions (May et al., 2004; Sokol and Clarren, 1989; Warren and Foudin, 2001). EtOH-induced CNS damage is permanent and probably the most deleterious consequence of prenatal exposure to this agent.

Prenatal EtOH-induced damage to the developing neocortex results in deficits in executive functioning that interfere with the skills necessary for daily living activities (Mattson et al., 1999). This damage is thought, in part, to be the consequence of disruptions in cellular proliferation, migration, and neuronal survival (Miller, 1986, 1996). Naturally occurring cell death contributes to normal neocortical development and EtOH increases this process leading to neurodegeneration, particularly in layer II during the third trimester-equivalent of human development (Ikonomidou et al., 2000; Mooney and Napper, 2005). Acute EtOH exposure at PD7 induces widespread neurodegeneration that spans numerous neocortical subdivisions, with variable sensitivity among cortical laminae (Ikonomidou et al., 2000). It has been proposed that EtOH-induced neurodegeneration results from a dual mechanism involving $GABA_A$ receptor ($GABA_AR$) potentiation and NMDA receptor (NMDAR) inhibition, which ultimately causes excessive neuronal inhibition (Ikonomidou et al., 2000; Olney et al., 2002b; Olney et al., 2004).

In preparations from relatively mature animals, the most consistent action of EtOH on NMDARs has been found to be inhibitory (Lovinger, 1996; Lovinger et al., 1989). However, it was recently demonstrated that EtOH has little postsynaptic effects on NMDARs in developing CA3 hippocampal pyramidal neurons (Mameli et al., 2005). GABA is the principal inhibitory neurotransmitter in the mature neocortex and it has been shown that EtOH enhances postsynaptic $GABA_AR$ function (Weiner and Valenzuela, 2006). Results obtained with preparations from different brain regions indicate that EtOH also enhances GABAergic function, at least in part, presynaptically (Carta et al., 2004; Roberto et al., 2003; Sanna et al., 2004; Weiner and Valenzuela, 2006). This presynaptic mechanism of action of EtOH has also been observed in developing neurons of the CA3 hippocampal region (Galindo et al., 2005).

In immature neurons, GABA depolarizes E_m as a consequence of increased $[Cl^-]_i$, which causes E_{Cl}^- to shift to less negative values than the resting membrane potential (Ben-Ari, 2002; Ben-Ari et al., 2007). Increased $[Cl^-]_i$ has been detected during the first postnatal week in the neocortex (Dammerman and Kriegstein, 2000; Garaschuk et al., 2000; Owens et al., 1999). $[Cl^-]_i$ is dependent on the expression of the Cl^- co-transporters NKCC1 (Cl^- importer) and KCC2 (Cl^-exporter). Although there is a reversed gradient for Cl^- flux during development, GABA exerts both excitatory and inhibitory actions because $GABA_AR$ opening can decrease the membrane resistance and shunt glutamatergic excitatory postsynaptic potentials (reviewed in Ben-Ari, 2002). Moreover, $GABA_AR$-induced

membrane depolarization can inactivate Na^+ channels (Zhang and Jackson, 1995). Importantly, $GABA_AR$-dependent $[Ca^{2+}]_i$ elevations have been shown to trigger cell death in developing neurons (Nunez et al., 2003).

In light of this evidence, we hypothesized that acute EtOH exposure could damage neocortical layer II neurons in PD 7–9 rats, by increasing GABA release resulting in excitation of these neurons, while having no effect on NMDAR activity. To test this hypothesis, we used the acute brain slice preparation, where we measured EtOH's effect on GABAergic transmission and characterized the effects of $GABA_AR$ activation on neuronal excitability. We also studied modulation of glutamatergic transmission and $[Ca^{2+}]_i$ by EtOH.

Materials and methods

For all experiments, timed-pregnant Sprague-Dawely rats (gestational days 14–18) were obtained from Harlan (Indianapolis, IN) and allowed to give birth at the UNM-HSC Animal Resource Facility. Neonatal offspring from these rats were used in these experiments. All animal procedures were approved by the UNM-Health Sciences Center Institutional Animal Care and Use Committee and conformed to National Institutes of Health Guidelines.

Preparation of acute slices

Unless indicated, all chemicals were from Sigma-Aldrich (St. Louis, MO). Coronal slices were prepared from the brains of PD 7–9 Spraque-Dawley male rats, as previously described (Galindo et al., 2005). Briefly, slices containing the parietal cortex, were cut at 400 μm in ice-cold cutting solution, and transferred to artificial cerebrospinal fluid (ACSF) at 35–36 °C for 45 minutes and stored at room temperature. Slices were then transferred to a recording chamber at 33° C and perfused with ACSF at a rate of 2 ml/min. Rats were decapitated under deep anesthesia with ketamine (250mg/kg/ I.P.). This agent blocks NMDARs and enhances $GABA_A$ Rs (Hevers et al., 2008; Lin et al., 1992). Ketamine anesthesia (~60 min duration) has been shown to induce apoptotic neurodegeneration in P7 mice 5 hours after injection (Young et al., 2005). In our study, animals were decapitated immediately after induction of anesthesia (2–3 min after ketamine injection) and slices were prepared in cutting solution containing ketamine (100 μg/ml), which takes ~10 min. Using this procedure, we consistently obtain healthy slices from neonatal animals, in agreement with the literature (Aitken et al., 1995). Thus, brief exposure to ketamine appears to have a neuroprotective action under our experimental conditions.

Whole-cell voltage-clamp electrophysiology

Whole-cell voltage-clamp electrophysiological recordings were performed under infrared-differential interference contrast (IR-DIC) microscopy with an Axopatch 200B amplifier (Molecular dynamics, Union City, CA). Patch-clamp electrodes had resistances of 4–8 MΩ. Unless otherwise indicated, voltage-clamp recordings were obtained at a holding potential of −65 mV. $GABA_AR$-dependent spontaneous postsynaptic currents ($GABA_A$-sPSCs) were recorded from layer II and layer III pyramidal neurons using two different internal solutions. Internal solution #1 contained (in mM): 140 CsCl, 10 HEPES, 1 EGTA, 4 MgATP, 0.4 MgGTP, and 2 mM QX-314 (pH 7.3). Internal solution #2 contained: (in mM), 145 KCl, 8 NaCl, 0.2 $MgCl_2$, 2 EGTA, 10 HEPES, 10 MgATP, 0.3 MgGTP, and 2 mM QX-314 (pH 7.2). Similar results were obtained with these internal solutions; therefore data were pooled. $GABA_A$-sPSCs were pharmacologically isolated using 3 mM kynurenic acid in the ACSF. Access resistances were between 15 and 40 MΩ; if the access resistance changed by more than 20%, the recording was discarded. Data were analyzed using Minis Analysis Program (Synaptosoft, Decatur, GA). Each slice was exposed once to 70 mM EtOH and recordings

were discarded if the frequency did not return to at least 50% of baseline following the washout of EtOH. The Kolmorgorov-Smirnov test (KS-test) was used to test each recording for a significant effect of treatment; $p < 0.01$ was considered to be significant. Pooled data were analyzed by one-way ANOVA followed by Dunnett's *post-hoc* test, and the control and washout conditions were averaged for each individual trace and the percent change as compared to EtOH was analyzed by a one-sample t-test using Prizm 4 (GraphPad Software, San Diego, CA).

Whole-cell AMPA receptor-dependent sPSCs (AMPA-sPSCs) were recorded from pyramidal neurons using internal solution #3 (in mM): 135 K-gluconate, 5 KCl, 10 HEPES, 0.2 EGTA, 4.6 $MgCl_2$, 4.0 Na_2ATP, 0.4 NaGTP and 2 mM QX-314 (pH 7.35). AMPA-sPSCs were pharmacologically isolated using a combination of 100 μM DL-2-amino-5-phosphonovaleric acid (DL-APV), 10 μM gabazine, and 50 μM picrotoxin (all from Tocris, Ellisville, MO) in the ACSF.

A pneumatic picopump (World Precision Instruments, Sarasota, FL) was used to apply puffs of 500 μM NMDA in the presence of TTX, 10 μM NBQX, 50 μM picrotoxin and 10 μM gabazine ($V_{holding} = -20$ mV). The puffing pipette was placed ~200 μm away from the patched neuron to produce a sub-maximal response. The pressure was set at 7 psi and the puff duration was 100 ms. Recording electrodes were filled with internal solution #3.

Perforated-patch electrophysiology

To determine the E_{Cl}^-, perforated-patch electrophysiological recordings were performed in layer II and layer III pyramidal neurons. A gramicidin stock solution was made fresh daily (5 mg/ml in dimethylsulfoxide). The stock solution was sonicated for ~ 30 min, then continuously vortexed at a low speed for the duration of the recording session. The tips of the microelectrodes, with resistances between 4–8 MΩ, were prefilled with internal solution #4 containing (in mM), 135 KCl, 10 HEPES, 2 $MgCl_2$, 5 Na-EGTA, and 0.5 $CaCl_2$ adjusted to pH 7.2 with KOH and then backfilled with the same internal solution containing 10 μg/ml of gramicidin. The access resistance was used to monitor the progression of perforation, which was considered to be completed when it was < 80 MΩ. In voltage-clamp mode, currents were elicited by exogenously applying muscimol (300 μM; Tocris) every 30 s with a pneumatic picopump using the same parameters described above. Muscimol-elicited currents were measured as the holding potential was changed in 20 mV increments from −100 mV to −20 mV. Muscimol elicited $GABA_A$R-currents were blocked using 50 μM picrotoxin and 10 μM gabazine. Peak current amplitudes were determined using Clampfit (Molecular Devices, Sunnyvale, CA) and any residual current remaining after application of these blockers was subtracted from the averaged peak amplitudes. A linear regression fit to the peak amplitudes as a function of membrane potential was determined using Prism, and the zero-current intercept was used to estimate E_{Cl}^-. Before determining E_{Cl}^-, the cell was switched from voltage-clamp to current-clamp ($I_{holding} = 0$) to estimate the resting membrane potential (E_m). Changes in action potential firing and E_m were determined in current-clamp mode, and 50 pA of current was injected every 30 s for 100 ms to elicit firing. Recordings were discarded if action potential number did not return to at least 50 % of baseline during EtOH washout.

Fluorometeric Ca^{2+} measurements

These measurements were performed in 400 μm slices loaded with fura-2 AM (Molecular Probes, Carlsbad, CA) in a recording chamber mounted on an upright microscope (Olympus BX51WI, Milville, NY) equipped with IR-DIC and a variable-scanning digital imaging system with Tillvision Ca^{2+} imaging software (T.I.L.L. Photonics GmBH, Eugene, OR). Background autoflourescence was determined at 350 nm, and then subtracted from each

acquisition time point for both 350 and 380 nm. Slices were incubated for 10 minutes at room temperature in oxygenated ACSF equilibrated with 95% O_2 and 5% CO_2 in 10 μM fura-2 AM in pluronic acid (0.1% DMSO). Slices where washed for 4 min, and then paired fluorescent measurements at 350 nm and 380 nm were made at an acquisition rate of 0.03 Hz from layer II/III pyramidal neurons in slices using a 40 × immersion lens. The recording sequence consisted of a 5-min baseline, a 10-min application of 30 μM muscimol, a 10-min washout period, and finally a 2.5-min application of 40 mM KCl. Only cells with responses to KCl were selected for analysis. Average 350 nm/380 nm ratios were measured for selected cells at each acquisition time point. EtOH exposed slices were corrected for a linearly decreasing baseline. Fluorescence values are given as a normalized value ($\Delta F/F_0$) × 100.

Fluorescence in situ hybridization (FISH) and immunohistochemistry

Six male rats were used for both FISH and immunohistochemistry for each of the following time periods: PD 3–4, 7–9, and 18–19, (total of 18 rats from 3 different litters). Rats were anesthetized with ketamine (250mg/kg/I.P.), rapidly decapitated, and brains were removed, quickly frozen in isopentane, equilibrated in a dry ice/ethanol slurry and stored at −80°C. Brains were formed into a block using Optimal Cutting Temperature (O.C.T.) reagent (Sakura Finetek, Torrance, CA) and 20 μm coronal sections containing the parietal cortex were prepared with a cryostat and collected on Superfrost-plus slides (VWR international, Westchester, PA) air-dried and stored at −80° C.

NKCC1 (clone ID 4824556, accession number BC033003) and KCC2 (clone ID 6838880, accession number BC054808) full-length cDNA plasmids were obtained from Open Biosystems (Huntsville, AL). Appropriate insertion of the clones was confirmed by sequencing (DNA Research Services, University of New Mexico, Health Sciences Center). The sequences were also checked to correspond to those in the rat genome database using the Basic Local Alignment Search Tool (www.ncbi.nlm.nih.gov/blast/Blast.cgi). Restriction endonucleases EcoR1 and Not1 were used to generate the template strand for *in vitro* transcription of the antisense strand of NKCC1 and Kpn1 for the sense strand (New England Biolabs Inc., Ipswich, MA). Templates for *in vitro* transcription of the antisense and sense strand for KCC2 were generated using AscI and PacI. The restriction digestion reactions were incubated for 2 hours at 37°C. FISH for NKCC1 and KCC2 was performed as previously described (Guzowski et al., 1999). Briefly, digoxigenin-labeled KCC2 and NKCC1 antisense and sense riboprobes were generated from linear cDNA using a commercially available transcription kit (Maxiscript; Ambion, Austin, TX) and premixed RNA digoxigenin labeled nucleotides using T3 or T7 polymerases (Roche Molecular Biochemicals, Palo Alto, CA). Products of the predicted size were observed in an RNA gel. Hybridization of NKCC1 or KCC2 digoxigenin-labeled riboprobes (1 ng/μl) was performed overnight at 56° C, followed by incubation with anti-digoxigenin horseradish peroxidase-conjugated antibodies (1:200 overnight at 4° C; Roche Molecular Biochemicals, Palo Alto, CA). TSA-cyanine-3 (Cy3) (1:50; PerkinElmer, Waltham, MA) was used to detect the horseradish peroxidase conjugate. Nuclei were counterstained with 4’,6’-diamidino-2-phenylindole (DAPI) (1:500; Invitrogen, Carlsbad, CA).

For immunohistochemistry, brains were cut into a block, fixed in 4% paraformaldehyde for 24 hours at 4° C, rinsed in phosphate buffered saline (PBS; pH 7.4) and then cryoprotected in 30% sucrose (wt/v) in PBS for 48 hours. Brains were quickly frozen in O.C.T. and coronal sections (14–18 μm) were collected on Superfrost-plus slides. Sections were air dried at room temperature and stored at −80°C. For KCC2, sections were brought to room temperature and rinsed in PBS, permeabilized with 0.1% Triton-X 100 (v/v) and then incubated in 1% bovine serum albumin (BSA) in PBS for 30 minutes. Sections were incubated overnight with a polyclonal anti-KCC2 antibody (1:200; Millipore, Billerica,

MA), in 1% bovine serum albumin in PBS. Sections were rinsed three times in PBS containing Tween-20 (0.05%; v/v) and incubated at room temp for two hours using an anti-rabbit CY3-conjugated secondary antibody (1:1000, Molecular probes, Carlsbad, CA). Nuclei were counterstained with DAPI (1:500). For NKCC1, sections were processed similarly to KCC2 with the exception that antigens were retrieved in 1% sodium dodecyl sulfate and 8% 2-mercaptoethanol in PBS for 5 min, following the initial wash in PBS (as previously described in Sung et al., 2000). Sections were washed in PBS and then incubated overnight at 4° C with a polyclonal anti-NKCC1 antibody in 1% BSA in PBS (1:200 Millipore, Billerica, MA). Sections were incubated with a polyclonal anti-rabbit Cy3 antibody under the same conditions as for KCC2. To exclude non-specific staining from the secondary-antibody, control sections were tested in the absence primary antibodies.

FISH and immunohistochemistry images were acquired with a Nikon TE2000U epifluorescence microscope (Melville, NY) with a 40 × oil immersion lens and captured using a CoolSNAP-Hq CCD camera (Roper Scientific, Tucson, AZ). A single optimized acquisition exposure time was determined for KCC2 using PD 18–19 tissue and for NKCC1 using PD 3–4 tissue (i.e. where there is highest expression of each co-transporter). These exposure times were also used to collect images at other ages. Images were analyzed using METAMORPH software (Universal Imaging, Sunnyvale, CA). For FISH analysis, DAPI images were used to identify nuclei; only cells displaying large, diffuse nuclei were considered for analysis because these presumably correspond to neurons (Guzowski and Worley, 2001). The regions of interest were transferred to a color-combined image of DAPI and Cy3, and the number of pyramidal nuclei expressing intranuclear RNA foci was counted as positive. For each section, two images were acquired per hemisphere in layer II/III of the parietal cortex. The number of positive intranuclear foci was averaged for a total of 16 images (3 sections per animal), and this was considered an n=1. We detected no intranuclear mRNA foci expression at PD 3–4, when the tissue was hybridized either with the NKCC1 sense strand or at PD 18–19 when the tissue was hybridized with the KCC2 sense strand.

For immunohistochemistry, KCC2 images were quantified using line scan analysis because there was expression of KCC2 throughout the neuropil in layer II/III. The average pixel intensity from 4 line scans aligned through layer II/III of the neocortex was collected per field. Four fields (2 fields per hemisphere) were used per section, and an average of data obtained in three sections was considered an n=1. For NKCC1, cells were counted positive if Cy3 expression was detected within or around the DAPI identify nuclei.

Data collected for FISH and immunohistochemistry were statistically analyzed using repeated measures one-way ANOVA, followed by a Tukey's *post-hoc* test.

Results

Acute EtOH increases $GABA_A$-sPSC frequency in layer II but not layer III pyramidal neurons at PD 7–9

In the developing rat neocortex, layers II and III cannot be easily distinguished, and have been considered a single layer that is commonly referred to as layer II/III (Fig 1A). However, when visualizing layer II/III in the acute slice with IR-DIC microscopy, we observed qualitative differences between pyramidal neurons within layer II/III. As had been previously noted (Suzuki and Bekkers, 2007), layer II neurons, which are located closer to the pial surface, are relatively smaller and are found in clusters, while layer III neurons had larger somas and were more loosely packed (Fig 1B). We also detected electrophysiological differences between neurons in these layers, in general agreement with a previous report (Bureau et al., 2004). Layer III neurons had a significantly larger capacitance and shorter

action potential rise time than layer II neurons (Table 1). We compared the acute affects of EtOH on GABAergic transmission in layer II vs. layer III neurons with these characteristics.

We used the whole-cell voltage-clamp configuration to record $GABA_A$ - sPSCs isolated with kynurenic acid (3 mM) in layer II pyramidal neurons at PD 7–9. We chose an EtOH concentration of 70 mM (0.32 g/dl) because it is in the range that was reported to trigger EtOH-induced neurodegeneration in layer II neocortical neurons (Ikonomidou et al., 2000). Acute exposure (10 min) to 70 mM EtOH in layer II pyramidal neurons reversibly increased the frequency of $GABA_A$-sPSCs (Fig 2A, C, $p< 0.05$ by repeated measures one-way ANOVA followed by Dunnett's *post-hoc* test vs. the 3 min time point, n=8 cells). $GABA_A$-sPSCs frequency returned to baseline levels within 5 minutes following termination of EtOH application. On average, there was a significant change in frequency (173.57 ± 21.04% of average of baseline and washout; n=8 cells; $p<0.01$ by one-sample t-test). EtOH significantly (KS-test, $p<0.01$) increased the frequency in 5 out of 8 cells. Fig 2B shows representative average traces at a more expanded time scale, illustrating that acute application of EtOH has no effect on $GABA_A$–sPSC amplitude or half-width. Repeated measures one-way ANOVA followed by Dunnett's *post-hoc* test did not reveal statistically significant differences in the amplitude or half-width timecourses in the absence vs. the presence of EtOH ($p> 0.05$, n=8 cells; not shown). There was no significant change in amplitude (100.53 ± 6.34% of average of baseline and washout; n=8 cells; $p>0.05$ by one-sample t-test) or half-width of $GABA_A$-sPSCs (101.19 ± 1.9 % of average of baseline and washout; n=8 cells; $p>0.05$ by one-sample t-test). EtOH significantly (KS-test, $p<0.01$) increased the amplitude in 3 out of 8 cells and decreased it in 2 out of 8 cells. EtOH significantly (KS-test, $p<0.01$) decreased the half-width in 1 out of 8 cells.

In layer III pyramidal neurons, 70 mM EtOH did not significantly increase the frequency of $GABA_A$-sPSCs (Fig 2D, F; $p > 0.05$; by repeated measures one-way ANOVA followed by Dunnett's *post-hoc* test, n=8 cells). There was no significant change in frequency (111.43 ± 12.64% of average of baseline and washout; n=8 cells; $p>0.05$ by one-sample t-test). EtOH significantly (KS-test, $p<0.01$) increased the frequency in 1 out of 8 cells and decreased the frequency in 2 out of 8 cells. Fig 2E shows representative average traces at a more expanded time scale, illustrating that EtOH has no effect on the amplitude or half-width. Repeated measures one-way ANOVA followed by Dunnett's *post-hoc* test did not reveal statistically significant differences in the amplitude or half-width timecourses in the absence vs. the presence of EtOH ($p> 0.05$, n=8 cells; not shown). There was no significant change in amplitude (96.94 ± 4.19 % of average of baseline and washout; n=8 cells; $p>0.05$ by one-sample t-test) or half-width of $GABA_A$-sPSCs (98.23 ± 2.9 % of average of baseline and washout; n=8 cells; $p>0.05$ by one-sample t-test). EtOH significantly (KS-test, $p<0.01$) increased the amplitude in 1 out of 8 cells and decreased it in 2 out of 8 cells. EtOH significantly (KS-test, $p<0.01$) increased the half-width in 2 out of 8 cells. As expected, $GABA_A$-sPSCs were blocked by 20 μM bicuculline in both layer II and layer III pyramidal neurons (n=3 for each layer; data not shown)

Acute application of EtOH has no significant effect on E_m or action potential number in layer II or layer III pyramidal neurons at PD 7–9

We used the perforated-patch current-clamp configuration to investigate the effect of acute application of 70 mM EtOH on E_m and the number of action potentials generated in response to a 50 pA current injection for 100 ms. Fig 3A–B show that during 5 min bath application of EtOH there was only minimal depolarization and no change in the number of action potentials generated in layer II and layer III pyramidal neurons ($p> 0.05$, n=7–8 cells). As a control, muscimol (30 μM) was bath-applied at the end of the recording, resulting in depolarization of E_m and elimination of action potential generation ($p< 0.001$ by repeated measures one-way ANOVA followed by Tukeys *post-hoc* test, n=7–8 cells). Furthermore, in

the presence of the $GABA_AR$ antagonists, picrotoxin and gabazine, there was no significant change in E_m or action potential number during bath application of EtOH or muscimol (Fig 3C–D; $p > 0.05$, repeated measures one-way ANOVA followed by Tukeys *post-hoc* test).

Acute application of muscimol causes a small, but significant increase in $[Ca^{2+}]_i$ in layer II/III neurons at PD 7–9

Since application of muscimol significantly depolarized E_m and attenuated the generation of action potentials in both layer II and layer III neurons, we assessed whether application of muscimol induced changes in $[Ca^{2+}]_i$ in layer II/III neurons as a population. Regions of interest were chosen for neurons covering a field that was restricted to layer II/III. However, because the optical resolution of the fluorescent image was less than that of the IR-DIC image used for patch clamping, it was impossible to accurately demark the boundary between layers II and III. Fig 4A represents the normalized average change in $\Delta F/F_0$ with respect to time, and as shown in this figure, there is a small $[Ca^{2+}]_i$ increase during the 10 min muscimol (30 μM) application. The increased $[Ca^{2+}]_i$ levels returned to near baseline during washout. As a control, KCl (40 mM) was added at the end of each recording and it produced the expected increase in $\Delta F/F_0$. As shown in Fig 4B, application of muscimol resulted in a small but significant increase in $[Ca^{2+}]_i$ ($p < 0.03$, one-sample *t*-test vs. zero, n=5 animals). KCl induced a ~17-fold greater change in the ratio of $\Delta F/F_0$ as compared with muscimol ($p < 0.0073$ by two-tailed paired *t*-test, n=5 animals).

E_{Cl}^- in layer II and layer III pyramidal neurons at PD 7–9

We next measured E_{Cl}^- in layer II and layer III pyramidal neurons, because there was a significant depolarization of E_m in both layers during muscimol application and a minimal increase in $[Ca^{2+}]_i$, suggesting that E_{Cl}^- in these neurons is shifted to a less negative value than E_m. Therefore, using the perforated patch technique, we measured E_{Cl}^- in layer II and III neurons in relation to the estimated E_m in the same neuron. E_{Cl}^- was determined by pressure application of muscimol (300 μM) onto PD 7–9 pyramidal neurons, in the presence of kynurenic acid (3 mM) to block ionotropic glutamate receptors. Fig 5A and C are representative traces for voltage steps between −20 and −100 mV for layer II and layer III pyramidal neurons and the resultant I–V curves are shown in Figs 5B and D; E_{Cl}^- was determined as the zero current intercept of the linear regression fit to the peak current data and the independently-estimated E_m for both cell types is indicated. In the majority of the cells (Fig 5E, 9 out of 12 cells), the E_{Cl}^- was shifted to a less negative value than E_m. In two layer III neurons, E_{Cl}^- was shifted to a more negative value than E_m, and in one layer II neuron $E_m = E_{Cl}^-$.

Expression of NKCC1 and KCC2

Since muscimol depolarizes E_m and the majority of layer II and layer III neurons have an E_{Cl}^- that is shifted to a less negative value than E_m, we investigated the protein expression of the Cl^- co-transporters, NKCC1 and KCC2, in layer II/III neocortical neurons at PD 7–9. For comparison, we determined expression of these co-transporters at PD 3–4 and PD 18–19. NKCC1 protein expression was evident at all developmental time points (Fig 6A1–A3), but the percent of NKCC1 protein expressing neurons was greatest (~90%) at PD 3–4 decreasing to ~ 50% at PD 7–9 and ~24 % at PD 18–19 (Fig 6B). The staining pattern observed at all ages was nuclear and cytoplasmic, as indicated by an orthogonal projection from a Z-stack image obtained at PD 7–9 (not shown).

Because the nuclear NKCC1 protein staining could be artifactual, we used FISH to measure the mRNA expression of this co-transporter in layer II/III neocortical neurons (Fig 6). Although intranuclear foci of NKCC1 mRNA expression were evident at all developmental time points (Fig 6A4–A6), a high percent (~90%) of neurons containing NKCC1 (+) mRNA

intranuclear foci were detected at PD 3–4 and this percent decreased significantly to ~70% at PD 7–9 and ~45% PD 18–19 (Fig 6C).

The expression pattern for KCC2 protein differed markedly from that of NKCC1 (Fig 7A1–A3). Expression of KCC2 was detectable throughout the neuropil in layer II/III neocortical neurons at all developmental ages with the smallest expression (1 arbitrary intensity unit/# cells per field) at PD 3–4 and subsequent increases to ~2.5 arbitrary intensity units/# cells per field at PD 7–9 and ~ 8 arbitrary intensity units/# cells per field at PD 18–19 (Fig 7B).

The mRNA expression for KCC2 in layer II/III neocortical neurons is shown in Fig 7A4–A6. Intranuclear mRNA foci expression was evident at all developmental time points, with the number of neurons containing KCC2 (+) mRNA intranuclear foci increasing significantly from ~20% at PD 3–4 to ~60% and ~90 % at PD 18–19 (Fig 7C).

Acute application of EtOH had no significant effect on currents evoked by exogenous application of NMDA in layer II or layer III pyramidal neurons at PD7–9

It has been postulated that acute EtOH exposure damages layer II neurons, in part, via NMDAR inhibition (Ikonomidou et al., 2000). Therefore, we investigated EtOH's effects on NMDAR function in layer II and layer III pyramidal neurons. Pressure application of NMDA (500 μM) in the presence of TTX (0.5 μM), gabazine (10 μM), picrotoxin (50 μM), and NBQX (10 μM) caused inward currents that were eliminated by MK-801 (10 μM)(Fig 8). Acute 5 minute exposure to 70 mM EtOH had no significant effect on the peak amplitude of NMDA-evoked currents in either layer II (n=10 cells) or layer III (n=6 cells) neurons as compared to control (Fig 8; $p>0.05$ by two-way ANOVA).

Acute EtOH did not affect AMPA-sPSC frequency or amplitude in layer II or layer III pyramidal neurons at PD 7–9

Fig 9A and D represent the lack of change of AMPA-sPSC frequency during acute 10 min application of 70 mM EtOH in either layer II or layer III pyramidal neurons. Fig 9B and E are representative average traces at a more expanded time, illustrating that acute application of EtOH had no effect on AMPA–sPSC amplitude or half-width. Neither in layer II (n = 11) nor layer III (n = 11) neurons did EtOH have any significant effect on the AMPA-sPSC frequency (Fig 9C, F, $p > 0.05$, by one-way ANOVA followed by Dunnett's *post-hoc* test). On average, there was no significant change in frequency (layer II: 100.75 ± 9.29 % of average of baseline and washout; n=11 cells or layer III: 130.1 ± 18.42 % of average of baseline and washout; n=11 cells; $p>0.05$ by one-sample t-test). EtOH significantly (KS-test, $p<0.01$) increased the frequency in 1 out of 11 cells and decreased the frequency in 2 out of 11 cells in layer II. EtOH significantly (KS-test, $p<0.01$) increased the frequency in 4 out of 11 and decreased it in 1 out of 11 cells in layer III. On average, there was a small but significant decrease in amplitude in layer II (90 ± 1.96% of average of baseline and washout; $p<0.001$ by one-sample t-test; n = 11) but not in layer III (98.3± 3 % of average of baseline and washout; $p>0.05$ by one-sample t-test; n = 11). EtOH significantly (KS-test, $p<0.01$) decreased the amplitude in 6 out of 11 cells in layer II. EtOH significantly (KS-test, $p<0.01$) increased the amplitude in 2 out of 11 cells in layer III. On average, there was a small but significant decrease in half-width of AMPA-sPSCs in layer II (93.21 ± 2.10% of average of baseline and washout; $p<0.01$ by one-sample t-test; n=11) but not in layer III (98.7 ± 2.275% of average of baseline and washout; $p>0.05$ by one-sample t-test; n = 11). EtOH significantly (KS-test, $p<0.01$) decreased the half-width in 4 out of 11 cells in layer II. EtOH significantly (KS-test, $p<0.01$) increased the half-width in 1 out of 11 cells, and decreased it in 2 out of 11 cells in layer III. There was no significant effect of EtOH on the amplitude or half-width timecourses in layer II or III (not shown; $p>0.05$ by one-way

ANOVA). As expected, AMPAR-mediated sPSCs were blocked in the presence of NBQX in both layers (10 μM; n = 2 cells for each layer, data not shown).

Acute application of EtOH minimally increases $[Ca^{2+}]_i$ in layer II/III neurons at PD 7–9

Finally, we assessed the acute effect of EtOH on $[Ca^{2+}]_i$ in layer II/III neurons in the absence of any receptor or channel antagonists. As shown in Fig 10A, there was a small increase in the normalized average $\Delta F/F_0$ during the 10 min EtOH application and the increase in $[Ca^{2+}]_i$ levels did not return to baseline levels during the washout. As shown in Fig 10B, application of EtOH resulted in a small but significant increase in $[Ca^{2+}]_i$ ($p < 0.001$, one-sample t-test vs. zero, n=5 animals). KCl induced a ~16-fold greater change in the ratio of $\Delta F/F_0$ as compared with EtOH ($p < 0.001$ by two-tailed paired *t*-test, n=5 animals).

Discussion

A reduction in neuronal number is a common consequence of prenatal exposure to EtOH and experimental evidence suggests that many potential mechanisms are responsible for this effect. One mechanism, the excessive inhibition model, has received considerable attention in the literature. In this model, EtOH exposure during the third trimester-equivalent of human pregnancy induces widespread neurodegeneration in different brain regions, in part, through potentiation of the $GABA_AR$, with neocortical layer II being particularly sensitive (Ikonomidou et al., 2000). Here, we tested this model using an *in vitro* acute slice preparation and found that EtOH produces a small increase in spontaneous action potential-dependent GABA release in PD 7–9 pyramidal neurons in layer II but had no direct postsynaptic effect on the $GABA_AR$. We found that $GABA_ARs$ at PD 7–9 have a dual excitatory/ inhibitory function in pyramidal neurons in layers II and III of the parietal cortex. However, the EtOH-induced increase of GABAergic transmission in layer II was not sufficient to affect the excitability of these neurons. In the excessive inhibition model, EtOH is also postulated to act by inhibiting the NMDAR, yet we found no evidence that EtOH has a direct effect on these receptors in layer II or III pyramidal neurons. Collectively, our data suggest that acute EtOH-induced neurodegeneration in these neurons is not the result of excessive inhibition as a consequence of potentiation of the $GABA_AR$ or inhibition of the NMDAR.

EtOH increases spontaneous action potential-dependent GABA release in layer II but not layer III neurons without affecting postsynaptic $GABA_ARs$

We found that acute exposure to 70 mM EtOH increased $GABA_A$-sPSC frequency without affecting amplitude or half-width in layer II neurons in PD 7–9 rats. However, EtOH did not affect GABAergic transmission in layer III pyramidal neurons. Our finding that EtOH did not affect $GABA_A$-sPSC amplitude or half-width is inconsistent with the excessive inhibition model, which postulates that EtOH directly enhances $GABA_AR$ function. EtOH increased $GABA_A$ -sPSC frequency indicating that it increases spontaneous action potential-dependent GABA release at these neurons (Siggins et al., 2005). EtOH-induced increases in $GABA_A$-sPSC frequency have been demonstrated in various brain regions from developing and mature animals (Carta et al., 2004; Galindo et al., 2005; Li et al., 2006; Marszalec et al., 1998; Roberto et al., 2003; Sanna et al., 2004; Weiner and Valenzuela, 2006). Our observation that EtOH does not exert a direct effect on the $GABA_AR$ is in agreement with previous findings in cultured cortical neurons (Marszalec et al., 1998) as well as developing CA3 hippocampal pyramidal neurons and spinal motoneurons in acute slices (Ziskind-Conhaim et al., 2003; Galindo et al., 2005). However, it is possible that intracellular signaling pathways could have been disrupted in our whole cell recordings and this could have altered postsynaptic $GABA_AR$ sensitivity to EtOH (Ron, 2004).

We found an EtOH-induced increase in $GABA_A$-sPSC frequency in layer II but not layer III pyramidal neurons. One explanation for this observation could be that EtOH differentially affects interneuronal synaptic inputs to pyramidal neurons in these layers (Bureau et al., 2004). In the piriform cortex, GABAergic basket cells have been identified in both layer II and layer III, but these specifically target layer II pyramidal neurons (Ekstrand et al., 2001). Bipolar basket cells are also found in layer II and the upper portion of layer III, and it has been suggested that these interneurons provide inhibitory feedback to layer II (Suzuki and Bekkers, 2007). Additionally, layer II has a higher percentage of interneurons expressing parvalbumin as compared with calbindin, whereas the reverse is true for layer III (Kubota and Jones, 1993; Suzuki and Bekkers, 2007).

Recently, it was shown that in some subtypes of interneurons in layer II/III, the threshold for action potential generation was close to E_m, making these cells highly excitable (Rheims et al., 2008). An EtOH-induced increase in GABA release could result from an intrinsic mechanism whereby EtOH increases the frequency of spontaneous action potential firing in a subset of interneurons, as was previously shown in cerebellar Golgi cells (Carta et al., 2004). Future work will be required to determine whether specific interneuron subtypes have differential sensitivity to acute EtOH exposure in the developing neocortex.

Although not consistently observed in different laboratories (Borghese and Harris, 2007; Botta et al., 2007; Carta et al., 2004), EtOH has been shown to directly potentiate extrasynaptic $GABA_A$ receptors containing delta subunits in the dentate gyrus, thalamus and cerebellum (Fleming et al., 2007; Hanchar et al., 2005; Jia et al., 2008; Lovinger and Homanics, 2007; Mody, 2008). The presence of a tonic depolarizing GABAergic current in layer II and III neurons from neonatal rats has been described (Cancedda et al., 2007). Therefore, the possibility that EtOH directly or indirectly (i.e. via changes in GABA spillover) modulates extrasynaptic $GABA_A$ receptors in these neurons should be investigated in the future.

Muscimol induced activation of the $GABA_A$ R exerts a dual excitatory/inhibitory effect on layer II/III neurons, but EtOH does not affect their excitability

We found that activation of the $GABA_A$ R with muscimol results in a dual excitatory and inhibitory response in both layer II and III pyramidal neurons: E_m significantly depolarized during muscimol application and this inhibited the generation of action potentials. This response is $GABA_A$R mediated because, in the presence of blockers of this receptor, there was neither a significant depolarization of E_m nor a change in action potential number. The muscimol-induced depolarization of E_m is likely mediated by Cl^- efflux through the $GABA_A$R. The $GABA_A$R induced decrease of action potential firing could be a consequence of an increase in membrane conductance that shunts depolarizing inputs (Staley and Mody, 1992). Moreover, $GABA_A$R-induced E_m depolarization can be sufficient to inactivate a substantial fraction of Na^+ channels, thereby blocking action potential generation (Zhang and Jackson, 1995). Muscimol-induced $GABA_A$R E_m depolarization minimally increased $[Ca^{2+}]_i$ in agreement with previous reports (Fukuda et al., 1998; Yamada et al., 2004). The minimal increase in $[Ca^{2+}]_i$ observed in the presence of muscimol is not surprising given that it induced only a small depolarization of the E_m that would be only sufficient to slightly activate voltage-gated Ca^{2+} channels.

It has been postulated that GABAmimetic drugs induce neurodegeneration by potentiating $GABA_A$Rs and inducing excessive inhibition (Ikonomidou et al., 2000; Mennerick and Zorumski, 2000; Olney et al., 2002b; Olney et al., 2004). This effect was thought to occur secondarily to E_m hyperpolarization. Here, we found that muscimol did suppress action potential firing in layer II/III neurons; however, firing decreased as a result of depolarization of E_m. It was previously demonstrated that the EtOH-induced neurodegeneration pattern, as

determined by DeOlmos silver stain, in part mimics the pattern of neurodegeneration induced by GABAmimetic drugs (Ikonomidou et al., 2000). From this, it was postulated that EtOH-induces neurodegeneration, in part, by a mechanism similar to the action of GABAmimetic drugs (Ikonomidou et al., 2000; Olney et al., 2002b; Olney et al., 2004). Interestingly, we found that the EtOH-induced increase in action potential-dependent GABA release in layer II pyramidal neurons did not depolarize E_m or have any effect on action potential generation. These data suggest that EtOH and GABAmimetic drugs do not affect GABAergic transmission in a similar manner and that they likely induce neuroapoptosis by different mechanisms.

E_{Cl}^- is at a more depolarized level than E_m in layer II/III pyramidal neurons at PD 7–9

In layers II and III in PD 7–9 rats, we found the estimated E_{Cl}^- shifted to a less negative value than the estimated E_m in the majority of neurons, in agreement with the literature (Cancedda et al., 2007; Rheims et al., 2008). This shift of E_{Cl}^- is indicative of increased $[Cl^-]_i$, as is commonly found in immature neurons (Ben-Ari, 2002). Under these conditions, $GABA_AR$ activation at E_m would produce an inward current mediated by Cl^- efflux, ultimately resulting in E_m depolarization. It has been suggested that the perforated-patch technique estimates the E_m at a more depolarized potential (Rheims et al., 2008). If this indeed is the case, then our estimated E_m would be even more negative than the values shown here, additionally increasing the driving force for a $GABA_AR$ mediated depolarizing response.

$[Cl^-]_i$ is dependent on the expression and activity of the NKCC1 and KCC2 co-transporters (Achilles et al., 2007; Brumback and Staley, 2008). The NKCC1 co-transporter is thought to be responsible for increasing $[Cl^-]_i$ levels above the passive $[Cl^-]_i$ (Achilles et al., 2007). Early in development, it is thought that NKCC1 is the dominantly expressed transporter and as development progresses, there is up regulation of the KCC2 co-transporter. In general agreement with the literature, we found mRNA and protein expression for both co-transporters at PD 7–9, at a level that is intermediate between that of layer II/III neurons from PD 3–4 and PD 18–19 rats (Lu et al., 1999; Shimizu-Okabe et al., 2002; Wang et al., 2002). Our electrophysiological findings indicate that $[Cl^-]_i$ in PD 7–9 neurons are higher than the level expected for more mature neurons, suggesting that NKCC1 is the functionally dominant transporter in this immature cells. Assuming that PD 7–9 neurons express similar quantities of NKCC1 and KCC2, one possible mechanism accounting for this could be that some of the expressed KCC2 is in an inactive conformation at this developmental stage (Balakrishnan et al., 2003). Alternatively, it was recently demonstrated that KCC2 must oligomerize to become fully functional and this oligomerization process may be incomplete in PD 7–9 neurons (Blaesse et al., 2006).

The NKCC1 co-transporter is thought to be located within the plasma membrane. Under our experimental conditions, it was detected in both the cytoplasm and the nucleus. This staining pattern could be an artifact, resulting from the antigen retrieval procedure that must be used for the anti-NKCC1 antibody to recognize its target. However, with this particular antibody, we did find that NKCC1 protein expression decreased with age, in agreement with the literature, and we detected abundant expression in the choroid plexus in older animals as expected (unpublished observation) (Dzhala et al., 2005; Hubner et al., 2001; Plotkin et al., 1997). In addition, our FISH studies demonstrated that the mRNA expression decreased similarly with age, as did NKCC1 protein expression. These results are in agreement with previous findings for NKCC1 mRNA expression in the neocortex and other brain regions (Hubner et al., 2001; Lu et al., 1999; Plotkin et al., 1997; Shimizu-Okabe et al., 2002; Wang et al., 2002; Yamada et al., 2004).

A hypothesis that should be investigated in the future is that ethanol exposure during the third trimester-equivalent of human pregnancy alters expression of KCC2 and/or NKCC1, leading to changes in E_{Cl}^{-} and $GABA_A$ receptor function.

EtOH had no effect on NMDA currents or AMPA-sPSCs in layer II/III pyramidal neurons of PD 7–9 rats

Blockade of the NMDAR with MK-801 and other antagonists triggers widespread neurodegeneration in PD 7 rats as determined by the DeOlmos silver staining technique (Ikonomidou et al., 1999). Sensitivity to NMDAR blockade coincides with the period of synaptogenesis (i.e. brain growth spurt) in which neural networks begin to establish connections by extending axons to postsynaptic targets to form functional communicative synapses (Ben-Ari, 2002). It has previously been shown in cell culture that 10 μM MK-801 exacerbates neuronal cell death (Papadia et al., 2008) and we found that this concentration of MK-801 abolishes NMDA currents in layer II and III pyramidal neurons at PD 7–9. This finding suggests that robust inhibition of NMDAR function is required to trigger neurodegeneration.

During this same critical developmental time period, it was demonstrated that EtOH induces a widespread neurodegeneration pattern resembling that of MK-801, with layer II of the neocortex being particularly sensitive (Ikonomidou et al., 2000). From these results, it was postulated that EtOH-induced inhibition of the NMDAR was in part responsible for suppressing neuronal activity and inducing widespread neurodegeneration. We found that acute application of 70 mM EtOH had no direct effect on the NMDAR in layer II and III pyramidal neurons from PD 7–9 rats. These data suggest that EtOH does not trigger neurodegeneration through inhibition of the NMDAR, as previously proposed.

It has been consistently found that the NMDAR in mature neurons is inhibited by EtOH (Lovinger, 1997). However, evidence has emerged indicating that NMDARs in immature CA3 pyramidal neurons are not directly inhibited by EtOH (Mameli et al., 2005). One explanation for the low EtOH sensitivity of NMDARs expressed in these immature neurons is that their subunit composition differs from that of receptors present in mature neurons. In the cortex, NR2B is detected at birth and its expression increases progressively into adulthood whereas the NR2A subunit is undetectable at birth and its expression peaks during the third postnatal week (Sheng et al., 1994; Wenzel et al., 1997). Electrophysiological studies suggest that NMDARs expressed in immature and mature neurons of the somatosensory cortex contain NR2B and NR2A subunits, respectively (Carmignoto and Vicini, 1992; Crair and Malenka, 1995; Monyer et al., 1994; Wenzel et al., 1997). Thus, NMDARs expressed in these immature neurons were expected to be sensitive to acute EtOH exposure (Allgaier, 2002; Chu et al., 1995). One possible explanation for their insensitivity to EtOH in developing layer II/III pyramidal neurons could be the presence of NR3A or NR2D subunits in the receptor assembly (Chu et al., 1995; Jin et al., 2008; Sun et al., 1998). Alternatively, differences in the NMDAR phosphorylation state or its association with other proteins can render NMDARs insensitive to EtOH in these neurons (Ron, 2004). It should also be considered that synaptic and extrasynaptic NMDARs could have differential sensitivity to EtOH in developing layer II and III pyramidal neurons. This possibility was not addressed in our experiments with exogenous NMDA application. Future studies should investigate this issue.

Our finding that acute EtOH exposure lacks inhibitory effects on NMDARs does not eliminate the possibility that these receptors play a role in the pathophysiology of FASD. A number of studies have reproducibly found that blocking the NMDAR during EtOH withdrawal in neonatal rats attenuates behavioral deficits later in life (Barron et al., 2008; Lewis et al., 2007; Thomas et al., 2002; Thomas et al., 2004). However, the results of the

present study and those of Mameli et al (2005) suggest that NMDAR upregulation during withdrawal does not represent a compensatory effect that is initiated by acute direct inhibition of the receptor by EtOH. NMDAR upregulation may be a consequence of EtOH modulation of other membrane, cytoplasmic or nuclear factors. For example, treatment of cultured cortical neurons with 100 mM EtOH for 5 days decreases neuron-restrictive silencer factor levels and binding activity, while increasing activity of the NR2B promoter (Qiang et al., 2005).

Because we did not find a direct effect of EtOH on the NMDAR, we studied its effects on AMPA-sPSCs. We found that EtOH had no effect on AMPA-sPSC frequency in layer II or III pyramidal neurons in PD 7–9 rats. These results suggest that EtOH does not affect spontaneous action potential-dependent glutamate release in these neurons. These results are in contrast to our previous observation that EtOH reduces glutamatergic release via inhibition of presynaptic N-type voltage gated Ca^{2+} channels in immature CA3 hippocampal pyramidal neurons (Mameli et al., 2005). We also found that EtOH had little effect on AMPA-sPSC amplitude or half-width in layer II or III pyramidal neurons, which is in contrast with our previous findings in developing CA3 pyramidal neurons where it was demonstrated that EtOH inhibits postsynaptic AMPARs (Mameli et al., 2005). One explanation for this discrepancy is that there are differences in AMPAR subunit composition or posttranslational modifications between the layer II/III and CA3 pyramidal neurons (Wang et al., 2004).

Acute application of EtOH in the absence of receptor antagonists results in a minimal, but significant increase $[Ca^{2+}]_i$ in layer II/III at PD 7–9

We found that in the absence of any receptor antagonist, EtOH produced a small increase in $[Ca^{2+}]_i$ that was comparable to the increase in $[Ca^{2+}]_i$ demonstrated during muscimol application. Muscimol depolarized E_m in layer II/III pyramidal neurons, whereas EtOH did not, suggesting that the EtOH-induced increase of $[Ca^{2+}]_i$ is via a different mechanism than membrane depolarization. One possible explanation for the observed increase in $[Ca^{2+}]_i$ during EtOH application is that it is a consequence of increased release of Ca^{2+} from intracellular stores as a result of activation of the ryanodine or the inositol 1,4,5-triphosphate receptor (Machu et al., 1989; Mironov and Hermann, 1996). Alternatively, EtOH could alter the neuron's ability to buffer $[Ca^{2+}]_i$ or it could interfere with the reuptake of Ca^{2+} into intracellular stores (Diamond and Gordon, 1997). The increase in $[Ca^{2+}]_i$ could also result from conversion of EtOH to acetaldehyde, which has been shown to increase reactive oxygen species (ROS), which can interfere with mitochondrial regulation of cytoplasmic Ca^{2+} (Goodlett and Horn, 2001; Jelski et al., 2007; Kroemer, 1997; Melis et al., 2007). Importantly, the increase in Ca^{2+} could be a factor in triggering apoptotic pathways (Goodlett and Horn, 2001).

Conclusions

In this study, we provide evidence that is inconsistent with the excessive inhibition model of FASD. We found that acute EtOH neither had an effect on the excitability of layer II pyramidal neurons, nor did it inhibit the NMDAR or $GABA_AR$. We cannot rule out the possibility that EtOH-modulates these receptors during longer EtOH exposures such as those required to induce cell death (i.e. 60–120 min) (Olney et al., 2002a; Olney et al., 2004; Tenkova et al., 2003). However, the data suggest that EtOH induces neuronal cell death by means of a different mechanism than that of NMDAR antagonists and GABA-mimetic drugs. One possibility is that EtOH-induced cell death is triggered by increased oxidative stress (Goodlett and Horn, 2001). EtOH decreases antioxidants, thus decreasing the cell's ability to break down the production of ROS that result from the metabolism of EtOH; oxidative stress can induce cell death by triggering necrosis and apoptotic pathways

(Goodlett and Horn, 2001; Martin, 2001). It has previously been demonstrated that ROS increases within minutes following EtOH application in cortical cultures (Ramachandran et al., 2003). Increased oxidative stress can also result in energy deprivation in developing neurons that could result in enhanced excitotoxic injury (Johnston, 2005). Another possibility is that the observed EtOH-induced widespread neurodegeneration results from neuronal swelling and subsequent necrosis. Indeed, the silver staining technique used by Ikonomidou et al. (2000) recognizes both necrotic and apoptotic neurons. This is supported by a computer-based model, which found that the amount of cell death determined by staining for activated caspase-3 is less than that found using the DeOlmos silver staining method (Gohlke et al., 2005).

The amount of EtOH-induced cell death reported by Ikonomidou et al. (2000) is in contrast to that found in other studies, where the percent of cell death has been shown to be significantly more moderate and less widespread (Miller, 1996; Mooney and Miller, 2003; Mooney and Napper, 2005). As a matter of fact, it has been suggested that the amount of EtOH-induced cell death reported by Ikonomidou et al. (2000) would result in neocortical collapse (Miller, 2006). The discrepancies between the results of these studies could be a consequence of the different experimental paradigms used to expose the animals to EtOH. Ikonomidou et al (2000) administered EtOH subcutaneously and the blood ethanol concentration reached 200 mg/dl (~43 mM) relatively rapidly (i.e. within 30 min) and then peaked at 500 mg/dl (~108 mM). It has been shown that intragastric administration of a dose of EtOH that produces blood ethanol concentrations near 274 mg/dl (60 mM) at a more slow rate (i.e. within 90 min) does not produce widespread neurodegeneration (Mooney and Napper, 2005).

It has been proposed that excessive inhibition-induced neurodegeneration during the third trimester equivalent is responsible for the deleterious cognitive effects seen in FASD (Olney et al., 2004). Using published results, a computer based model predicted that EtOH exposure during the second trimester equivalent would cause more severe neuronal loss in the neocortex than exposure during the third trimester-equivalent (Gohlke et al., 2005). This suggests that the second trimester-equivalent may be more sensitive to EtOH-induced neuronal loss. This is supported in the literature where it has been reported that second trimester-equivalent EtOH exposure disrupts the sequence of neurogenesis resulting in decreased neuronal numbers (Miller, 1986, 1996; Miller and Potempa, 1990). Second trimester-equivalent exposure has also been shown to increase the number of cortical GABAergic neurons, enhancing tangential migration to the neocortical laminar layers (Cuzon et al., 2008). Thus, future studies should examine the mechanism by which EtOH alters neocortical development using paradigms that include exposure during this critical period of gestation.

Acknowledgments

Supported by NIH grant #AA015614. Jennifer Sanderson was supported by funds from NIH training grant #AA014127 and NRSA pre-doctoral fellowship #AA016880-01.

References

Achilles K, Okabe A, Ikeda M, Shimizu-Okabe C, Yamada J, Fukuda A, Luhmann HJ, Kilb W. Kinetic properties of Cl uptake mediated by Na+-dependent K+-2Cl cotransport in immature rat neocortical neurons. J Neurosci 2007;27:8616–8627. [PubMed: 17687039]

Aitken PG, Breese GR, Dudek FF, Edwards F, Espanol MT, Larkman PM, Lipton P, Newman GC, Nowak TS Jr, Panizzon KL, et al. Preparative methods for brain slices: a discussion. J Neurosci Methods 1995;59:139–149. [PubMed: 7475244]

Allgaier C. Ethanol sensitivity of NMDA receptors. Neurochem Int 2002;41:377–382. [PubMed: 12213224]

Anderson SA, Marin O, Horn C, Jennings K, Rubenstein JL. Distinct cortical migrations from the medial and lateral ganglionic eminences. Development 2001;128:353–363. [PubMed: 11152634]

Balakrishnan V, Becker M, Lohrke S, Nothwang HG, Guresir E, Friauf E. Expression and function of chloride transporters during development of inhibitory neurotransmission in the auditory brainstem. J Neurosci 2003;23:4134–4145. [PubMed: 12764101]

Barron S, Mulholland PJ, Littleton JM, Prendergast MA. Age and gender differences in response to neonatal ethanol withdrawal and polyamine challenge in organotypic hippocampal cultures. Alcohol Clin Exp Res 2008;32:929–936. [PubMed: 18445110]

Ben-Ari Y. Excitatory actions of gaba during development: the nature of the nurture. Nat Rev Neurosci 2002;3:728–739. [PubMed: 12209121]

Ben-Ari Y. Basic developmental rules and their implications for epilepsy in the immature brain. Epileptic Disord 2006;8:91–102. [PubMed: 16793570]

Ben-Ari Y, Gaiarsa JL, Tyzio R, Khazipov R. GABA: a pioneer transmitter that excites immature neurons and generates primitive oscillations. Physiol Rev 2007;87:1215–1284. [PubMed: 17928584]

Blaesse P, Guillemin I, Schindler J, Schweizer M, Delpire E, Khiroug L, Friauf E, Nothwang HG. Oligomerization of KCC2 correlates with development of inhibitory neurotransmission. J Neurosci 2006;26:10407–10419. [PubMed: 17035525]

Borghese CM, Harris RA. Studies of ethanol actions on recombinant delta-containing gamma-aminobutyric acid type A receptors yield contradictory results. Alcohol 2007;41:155–162. [PubMed: 17521845]

Botta P, Radcliffe RA, Carta M, Mameli M, Daly E, Floyd KL, Deitrich RA, Valenzuela CF. Modulation of GABAA receptors in cerebellar granule neurons by ethanol: a review of genetic and electrophysiological studies. Alcohol 2007;41:187–199. [PubMed: 17521847]

Brumback AC, Staley KJ. Thermodynamic regulation of NKCC1-mediated Cl- cotransport underlies plasticity of GABA(A) signaling in neonatal neurons. J Neurosci 2008;28:1301–1312. [PubMed: 18256250]

Bureau I, Shepherd GM, Svoboda K. Precise development of functional and anatomical columns in the neocortex. Neuron 2004;42:789–801. [PubMed: 15182718]

Bystron I, Blakemore C, Rakic P. Development of the human cerebral cortex: Boulder Committee revisited. Nat Rev Neurosci 2008;9:110–122. [PubMed: 18209730]

Cancedda L, Fiumelli H, Chen K, Poo MM. Excitatory GABA action is essential for morphological maturation of cortical neurons in vivo. J Neurosci 2007;27:5224–5235. [PubMed: 17494709]

Carmignoto G, Vicini S. Activity-dependent decrease in NMDA receptor responses during development of the visual cortex. Science 1992;258:1007–1011. [PubMed: 1279803]

Carta M, Mameli M, Valenzuela CF. Alcohol enhances GABAergic transmission to cerebellar granule cells via an increase in Golgi cell excitability. J Neurosci 2004;24:3746–3751. [PubMed: 15084654]

Chu B, Anantharam V, Treistman SN. Ethanol inhibition of recombinant heteromeric NMDA channels in the presence and absence of modulators. J Neurochem 1995;65:140–148. [PubMed: 7540660]

Crair MC, Malenka RC. A critical period for long-term potentiation at thalamocortical synapses. Nature 1995;375:325–328. [PubMed: 7753197]

Cuzon VC, Yeh PW, Yanagawa Y, Obata K, Yeh HH. Ethanol consumption during early pregnancy alters the disposition of tangentially migrating GABAergic interneurons in the fetal cortex. J Neurosci 2008;28:1854–1864. [PubMed: 18287502]

Dammerman RS, Kriegstein AR. Transient actions of neurotransmitters during neocortical development. Epilepsia 2000;41:1080–1081. [PubMed: 10961650]

Diamond I, Gordon AS. Cellular and molecular neuroscience of alcoholism. Physiol Rev 1997;77:1–20. [PubMed: 9016298]

Dzhala VI, Talos DM, Sdrulla DA, Brumback AC, Mathews GC, Benke TA, Delpire E, Jensen FE, Staley KJ. NKCC1 transporter facilitates seizures in the developing brain. Nat Med 2005;11:1205–1213. [PubMed: 16227993]

Ekstrand JJ, Domroese ME, Feig SL, Illig KR, Haberly LB. Immunocytochemical analysis of basket cells in rat piriform cortex. J Comp Neurol 2001;434:308–328. [PubMed: 11331531]

Fleming RL, Wilson WA, Swartzwelder HS. Magnitude and ethanol sensitivity of tonic GABAA receptor-mediated inhibition in dentate gyrus changes from adolescence to adulthood. J Neurophysiol 2007;97:3806–3811. [PubMed: 17376852]

Fukuda A, Muramatsu K, Okabe A, Shimano Y, Hida H, Fujimoto I, Nishino H. Changes in intracellular Ca2+ induced by GABAA receptor activation and reduction in Cl- gradient in neonatal rat neocortex. J Neurophysiol 1998;79:439–446. [PubMed: 9425212]

Galindo R, Zamudio PA, Valenzuela CF. Alcohol is a potent stimulant of immature neuronal networks: implications for fetal alcohol spectrum disorder. J Neurochem 2005;94:1500–1511. [PubMed: 16000153]

Garaschuk O, Linn J, Eilers J, Konnerth A. Large-scale oscillatory calcium waves in the immature cortex. Nat Neurosci 2000;3:452–459. [PubMed: 10769384]

Gohlke JM, Griffith WC, Faustman EM. A systems-based computational model for dose-response comparisons of two mode of action hypotheses for ethanol-induced neurodevelopmental toxicity. Toxicol Sci 2005;86:470–484. [PubMed: 15917484]

Goodlett CR, Horn KH. Mechanisms of alcohol-induced damage to the developing nervous system. Alcohol Res Health 2001;25:175–184. [PubMed: 11810955]

Guerri C. Neuroanatomical and neurophysiological mechanisms involved in central nervous system dysfunctions induced by prenatal alcohol exposure. Alcohol Clin Exp Res 1998;22:304–312. [PubMed: 9581633]

Guillery RW. Is postnatal neocortical maturation hierarchical? Trends Neurosci 2005;28:512–517. [PubMed: 16126285]

Guzowski JF, McNaughton BL, Barnes CA, Worley PF. Environment-specific expression of the immediate-early gene Arc in hippocampal neuronal ensembles. Nat Neurosci 1999;2:1120–1124. [PubMed: 10570490]

Guzowski, JF.; Worley, PF. Cellular Compartment Analysis of Temporal Activity by Fluorescence In Situ Hybridization (catFISH). In: Gerfen, CR.; Holmes, A.; Rogawski, MA.; Sibley, D.; Skolnick, P.; Wray, S., editors. Current Protocols in Neuroscience. John Wiley & Sonsa, Inc; 2001. p. 1.8.1-1.8.16.

Hanchar HJ, Dodson PD, Olsen RW, Otis TS, Wallner M. Alcohol-induced motor impairment caused by increased extrasynaptic GABA(A) receptor activity. Nat Neurosci 2005;8:339–345. [PubMed: 15696164]

Hevers W, Hadley SH, Luddens H, Amin J. Ketamine, but not phencyclidine, selectively modulates cerebellar GABA(A) receptors containing alpha6 and delta subunits. J Neurosci 2008;28:5383–5393. [PubMed: 18480294]

Hubner CA, Lorke DE, Hermans-Borgmeyer I. Expression of the Na-K-2Cl-cotransporter NKCC1 during mouse development. Mech Dev 2001;102:267–269. [PubMed: 11287208]

Ignacio MP, Kimm EJ, Kageyama GH, Yu J, Robertson RT. Postnatal migration of neurons and formation of laminae in rat cerebral cortex. Anat Embryol (Berl) 1995;191:89–100. [PubMed: 7726396]

Ikonomidou C, Bittigau P, Ishimaru MJ, Wozniak DF, Koch C, Genz K, Price MT, Stefovska V, Horster F, Tenkova T, Dikranian K, Olney JW. Ethanol-induced apoptotic neurodegeneration and fetal alcohol syndrome. Science 2000;287:1056–1060. [PubMed: 10669420]

Ikonomidou C, Bosch F, Miksa M, Bittigau P, Vockler J, Dikranian K, Tenkova TI, Stefovska V, Turski L, Olney JW. Blockade of NMDA receptors and apoptotic neurodegeneration in the developing brain. Science 1999;283:70–74. [PubMed: 9872743]

Jelski W, Grochowska-Skiba B, Szmitkowski M. Alcohol dehydrogenase and the metabolism of ethanol in the brain. Postepy Hig Med Dosw (Online) 2007;61:226–230. [PubMed: 18364675]

Jia F, Chandra D, Homanics GE, Harrison NL. Ethanol modulates synaptic and extrasynaptic GABAA receptors in the thalamus. J Pharmacol Exp Ther 2008;326:475–482. [PubMed: 18477766]

Jin C, Smothers CT, Woodward JJ. Enhanced ethanol inhibition of recombinant N-methyl-D-aspartate receptors by magnesium: role of NR3A subunits. Alcohol Clin Exp Res 2008;32:1059–1066. [PubMed: 18445116]

Johnston MV. Excitotoxicity in perinatal brain injury. Brain Pathol 2005;15:234–240. [PubMed: 16196390]

Kroemer G. Mitochondrial implication in apoptosis. Towards an endosymbiont hypothesis of apoptosis evolution. Cell Death Differ 1997;4:443–456. [PubMed: 16465265]

Kubota Y, Jones EG. Co-localization of two calcium binding proteins in GABA cells of rat piriform cortex. Brain Res 1993;600:339–344. [PubMed: 8435756]

Levitt P, Eagleson KL, Powell EM. Regulation of neocortical interneuron development and the implications for neurodevelopmental disorders. Trends Neurosci 2004;27:400–406. [PubMed: 15219739]

Lewis B, Wellmann KA, Barron S. Agmatine reduces balance deficits in a rat model of third trimester binge-like ethanol exposure. Pharmacol Biochem Behav 2007;88:114–121. [PubMed: 17714770]

Li Q, Wilson WA, Swartzwelder HS. Developmental differences in the sensitivity of spontaneous and miniature IPSCs to ethanol. Alcohol Clin Exp Res 2006;30:119–126. [PubMed: 16433739]

Lin LH, Chen LL, Zirrolli JA, Harris RA. General anesthetics potentiate gamma-aminobutyric acid actions on gamma-aminobutyric acidA receptors expressed by Xenopus oocytes: lack of involvement of intracellular calcium. J Pharmacol Exp Ther 1992;263:569–578. [PubMed: 1331405]

Lovinger DM. Interactions between ethanol and agents that act on the NMDA-type glutamate receptor. Alcohol Clin Exp Res 1996;20:187A–191A.

Lovinger DM. Alcohols and neurotransmitter gated ion channels: past, present and future. Naunyn Schmiedebergs Arch Pharmacol 1997;356:267–282. [PubMed: 9303562]

Lovinger DM, Homanics GE. Tonic for what ails us? high-affinity GABAA receptors and alcohol. Alcohol 2007;41:139–143. [PubMed: 17521844]

Lovinger DM, White G, Weight FF. Ethanol inhibits NMDA-activated ion current in hippocampal neurons. Science 1989;243:1721–1724. [PubMed: 2467382]

Lu J, Karadsheh M, Delpire E. Developmental regulation of the neuronal-specific isoform of K-Cl cotransporter KCC2 in postnatal rat brains. J Neurobiol 1999;39:558–568. [PubMed: 10380077]

Machu T, Woodward JJ, Leslie SW. Ethanol and inositol 1,4,5-trisphosphate mobilize calcium from rat brain microsomes. Alcohol 1989;6:431–436. [PubMed: 2597345]

Mameli M, Zamudio PA, Carta M, Valenzuela CF. Developmentally regulated actions of alcohol on hippocampal glutamatergic transmission. J Neurosci 2005;25:8027–8036. [PubMed: 16135760]

Markram H, Toledo-Rodriguez M, Wang Y, Gupta A, Silberberg G, Wu C. Interneurons of the neocortical inhibitory system. Nat Rev Neurosci 2004;5:793–807. [PubMed: 15378039]

Marszalec W, Aistrup GL, Narahashi T. Ethanol modulation of excitatory and inhibitory synaptic interactions in cultured cortical neurons. Alcohol Clin Exp Res 1998;22:1516–1524. [PubMed: 9802537]

Martin LJ. Neuronal cell death in nervous system development, disease, and injury (Review). Int J Mol Med 2001;7:455–478. [PubMed: 11295106]

Mattson SN, Goodman AM, Caine C, Delis DC, Riley EP. Executive functioning in children with heavy prenatal alcohol exposure. Alcohol Clin Exp Res 1999;23:1808–1815. [PubMed: 10591598]

May PA, Gossage JP, White-Country M, Goodhart K, Decoteau S, Trujillo PM, Kalberg WO, Viljoen DL, Hoyme HE. Alcohol consumption and other maternal risk factors for fetal alcohol syndrome among three distinct samples of women before, during, and after pregnancy: the risk is relative. Am J Med Genet C Semin Med Genet 2004;127C:10–20. [PubMed: 15095467]

Melis M, Enrico P, Peana AT, Diana M. Acetaldehyde mediates alcohol activation of the mesolimbic dopamine system. Eur J Neurosci 2007;26:2824–2833. [PubMed: 18001279]

Mennerick S, Zorumski CF. Neural activity and survival in the developing nervous system. Mol Neurobiol 2000;22:41–54. [PubMed: 11414280]

Miller MW. Effects of alcohol on the generation and migration of cerebral cortical neurons. Science 1986;233:1308–1311. [PubMed: 3749878]

Miller MW. Effect of early exposure to ethanol on the protein and DNA contents of specific brain regions in the rat. Brain Res 1996;734:286–294. [PubMed: 8896836]

Miller MW. Brain development: Normal Processes and the effects of alcohol and nicotine. 2006

Miller MW, Potempa G. Numbers of neurons and glia in mature rat somatosensory cortex: effects of prenatal exposure to ethanol. J Comp Neurol 1990;293:92–102. [PubMed: 2312794]

Mironov SL, Hermann A. Ethanol actions on the mechanisms of Ca2+ mobilization in rat hippocampal cells are mediated by protein kinase C. Brain Res 1996;714:27–37. [PubMed: 8861606]

Mody I. Extrasynaptic GABAA receptors in the crosshairs of hormones and ethanol. Neurochem Int 2008;52:60–64. [PubMed: 17714830]

Monyer H, Burnashev N, Laurie DJ, Sakmann B, Seeburg PH. Developmental and regional expression in the rat brain and functional properties of four NMDA receptors. Neuron 1994;12:529–540. [PubMed: 7512349]

Mooney SM, Miller MW. Ethanol-induced neuronal death in organotypic cultures of rat cerebral cortex. Brain Res Dev Brain Res 2003;147:135–141.

Mooney SM, Napper RM. Early postnatal exposure to alcohol reduces the number of neurons in the occipital but not the parietal cortex of the rat. Alcohol Clin Exp Res 2005;29:683–691. [PubMed: 15834235]

Nunez JL, Alt JJ, McCarthy MM. A new model for prenatal brain damage. I. GABAA receptor activation induces cell death in developing rat hippocampus. Exp Neurol 2003;181:258–269. [PubMed: 12781998]

O'Leary DD, Chou SJ, Hamasaki T, Sahara S, Takeuchi A, Thuret S, Leingartner A. Regulation of laminar and area patterning of mammalian neocortex and behavioural implications. Novartis Found Symp 2007;288:141–159. discussion 159–164, 276–181. [PubMed: 18494257]

Olney JW, Tenkova T, Dikranian K, Muglia LJ, Jermakowicz WJ, D'Sa C, Roth KA. Ethanol-induced caspase-3 activation in the in vivo developing mouse brain. Neurobiol Dis 2002a;9:205–219. [PubMed: 11895372]

Olney JW, Wozniak DF, Jevtovic-Todorovic V, Farber NB, Bittigau P, Ikonomidou C. Drug-induced apoptotic neurodegeneration in the developing brain. Brain Pathol 2002b;12:488–498. [PubMed: 12408236]

Olney JW, Young C, Wozniak DF, Jevtovic-Todorovic V, Ikonomidou C. Do pediatric drugs cause developing neurons to commit suicide? Trends Pharmacol Sci 2004;25:135–139. [PubMed: 15019268]

Owens DF, Liu X, Kriegstein AR. Changing properties of GABA(A) receptor-mediated signaling during early neocortical development. J Neurophysiol 1999;82:570–583. [PubMed: 10444657]

Papadia S, Soriano FX, Leveille F, Martel MA, Dakin KA, Hansen HH, Kaindl A, Sifringer M, Fowler J, Stefovska V, McKenzie G, Craigon M, Corriveau R, Ghazal P, Horsburgh K, Yankner BA, Wyllie DJ, Ikonomidou C, Hardingham GE. Synaptic NMDA receptor activity boosts intrinsic antioxidant defenses. Nat Neurosci 2008;11:476–487. [PubMed: 18344994]

Parnavelas JG. The origin and migration of cortical neurones: new vistas. Trends Neurosci 2000;23:126–131. [PubMed: 10675917]

Plotkin MD, Snyder EY, Hebert SC, Delpire E. Expression of the Na-K-2Cl cotransporter is developmentally regulated in postnatal rat brains: a possible mechanism underlying GABA's excitatory role in immature brain. J Neurobiol 1997;33:781–795. [PubMed: 9369151]

Qiang M, Rani CS, Ticku MK. Neuron-restrictive silencer factor regulates the N-methyl-D-aspartate receptor 2B subunit gene in basal and ethanol-induced gene expression in fetal cortical neurons. Mol Pharmacol 2005;67:2115–2125. [PubMed: 15755907]

Ramachandran V, Watts LT, Maffi SK, Chen J, Schenker S, Henderson G. Ethanol-induced oxidative stress precedes mitochondrially mediated apoptotic death of cultured fetal cortical neurons. J Neurosci Res 2003;74:577–588. [PubMed: 14598302]

Rheims S, Minlebaev M, Ivanov A, Represa A, Khazipov R, Holmes GL, Ben-Ari Y, Zilberter Y. Excitatory GABA in Rodent Developing Neocortex in vitro. J Neurophysiol. 2008

Roberto M, Nelson TE, Ur CL, Brunelli M, Sanna PP, Gruol DL. The transient depression of hippocampal CA1 LTP induced by chronic intermittent ethanol exposure is associated with an inhibition of the MAP kinase pathway. Eur J Neurosci 2003;17:1646–1654. [PubMed: 12752382]

Ron D. Signaling cascades regulating NMDA receptor sensitivity to ethanol. Neuroscientist 2004;10:325–336. [PubMed: 15271260]

Sanna E, Talani G, Busonero F, Pisu MG, Purdy RH, Serra M, Biggio G. Brain steroidogenesis mediates ethanol modulation of GABAA receptor activity in rat hippocampus. J Neurosci 2004;24:6521–6530. [PubMed: 15269263]

Sheng M, Cummings J, Roldan LA, Jan YN, Jan LY. Changing subunit composition of heteromeric NMDA receptors during development of rat cortex. Nature 1994;368:144–147. [PubMed: 8139656]

Shimizu-Okabe C, Yokokura M, Okabe A, Ikeda M, Sato K, Kilb W, Luhmann HJ, Fukuda A. Layer-specific expression of Cl- transporters and differential [Cl-]i in newborn rat cortex. Neuroreport 2002;13:2433–2437. [PubMed: 12499844]

Siggins GR, Roberto M, Nie Z. The tipsy terminal: presynaptic effects of ethanol. Pharmacol Ther 2005;107:80–98. [PubMed: 15963352]

Sokol RJ, Clarren SK. guidelines for use of terminology describing the impact of prenatal alcohol on the offspring. Alcohol Clin Exp Res 1989;13:597–598. [PubMed: 2679217]

Staley KJ, Mody I. Shunting of excitatory input to dentate gyrus granule cells by a depolarizing GABAA receptor-mediated postsynaptic conductance. J Neurophysiol 1992;68:197–212. [PubMed: 1381418]

Sun L, Margolis FL, Shipley MT, Lidow MS. Identification of a long variant of mRNA encoding the NR3 subunit of the NMDA receptor: its regional distribution and developmental expression in the rat brain. FEBS Lett 1998;441:392–396. [PubMed: 9891978]

Sung KW, Kirby M, McDonald MP, Lovinger DM, Delpire E. Abnormal GABAA receptor-mediated currents in dorsal root ganglion neurons isolated from Na-K-2Cl cotransporter null mice. J Neurosci 2000;20:7531–7538. [PubMed: 11027211]

Suzuki N, Bekkers JM. Inhibitory interneurons in the piriform cortex. Clin Exp Pharmacol Physiol 2007;34:1064–1069. [PubMed: 17714095]

Tenkova T, Young C, Dikranian K, Labruyere J, Olney JW. Ethanol-induced apoptosis in the developing visual system during synaptogenesis. Invest Ophthalmol Vis Sci 2003;44:2809–2817. [PubMed: 12824217]

Thomas JD, Fleming SL, Riley EP. Administration of low doses of MK-801 during ethanol withdrawal in the developing rat pup attenuates alcohol's teratogenic effects. Alcohol Clin Exp Res 2002;26:1307–1313. [PubMed: 12198409]

Thomas JD, Garcia GG, Dominguez HD, Riley EP. Administration of eliprodil during ethanol withdrawal in the neonatal rat attenuates ethanol-induced learning deficits. Psychopharmacology (Berl) 2004;175:189–195. [PubMed: 15064913]

Wang C, Shimizu-Okabe C, Watanabe K, Okabe A, Matsuzaki H, Ogawa T, Mori N, Fukuda A, Sato K. Developmental changes in KCC1, KCC2, and NKCC1 mRNA expressions in the rat brain. Brain Res Dev Brain Res 2002;139:59–66.

Wang WW, Cao R, Rao ZR, Chen LW. Differential expression of NMDA and AMPA receptor subunits in DARPP-32-containing neurons of the cerebral cortex, hippocampus and neostriatum of rats. Brain Res 2004;998:174–183. [PubMed: 14751588]

Warren KR, Foudin LL. Alcohol-related birth defects-the past, present, and future. Alcohol Res Health 2001;25:153–158. [PubMed: 11810952]

Weiner JL, Valenzuela CF. Ethanol modulation of GABAergic transmission: the view from the slice. Pharmacol Ther 2006;111:533–554. [PubMed: 16427127]

Wenzel A, Fritschy JM, Mohler H, Benke D. NMDA receptor heterogeneity during postnatal development of the rat brain: differential expression of the NR2A, NR2B, and NR2C subunit proteins. J Neurochem 1997;68:469–478. [PubMed: 9003031]

Yamada J, Okabe A, Toyoda H, Kilb W, Luhmann HJ, Fukuda A. Cl- uptake promoting depolarizing GABA actions in immature rat neocortical neurones is mediated by NKCC1. J Physiol 2004;557:829–841. [PubMed: 15090604]

Young C, Jevtovic-Todorovic V, Qin YQ, Tenkova T, Wang H, Labruyere J, Olney JW. Potential of ketamine and midazolam, individually or in combination, to induce apoptotic neurodegeneration in the infant mouse brain. Br J Pharmacol 2005;146:189–197. [PubMed: 15997239]

Zhang SJ, Jackson MB. GABAA receptor activation and the excitability of nerve terminals in the rat posterior pituitary. J Physiol 1995;483 (Pt 3):583–595. [PubMed: 7776245]

Ziskind-Conhaim L, Gao BX, Hinckley C. Ethanol dual modulatory actions on spontaneous postsynaptic currents in spinal motoneurons. J Neurophysiol 2003;89:806–813. [PubMed: 12574458]

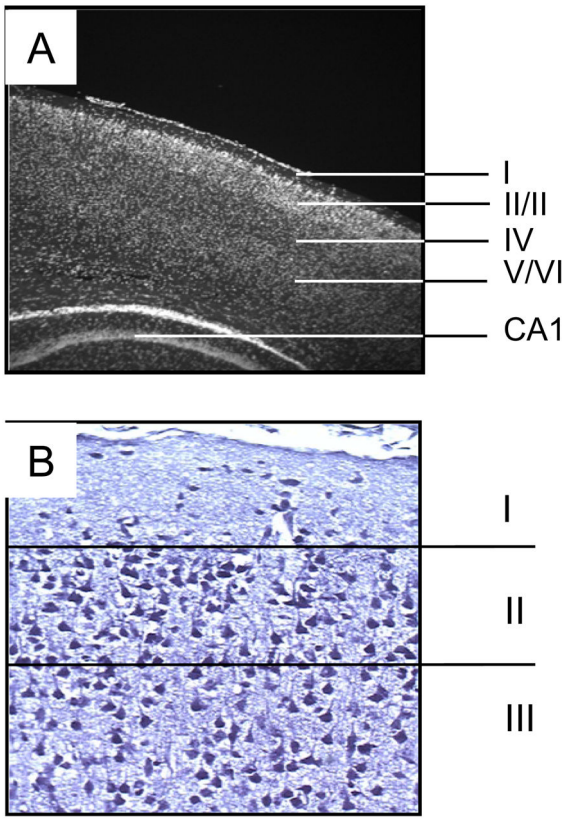

Figure 1. Histological characterization of neocortical layers in P7–9 rats

(A) 10× confocal images of coronal sections (14–18 μm) stained with the nuclear stain, DAPI. The six neocortical layers are identified along with the CA1 hippocampal region. (B) 20× light microscopy images of coronal sections (14–18 μm) stained with hematoxylin-eosin illustrating the characteristics of neurons in layers II and III.

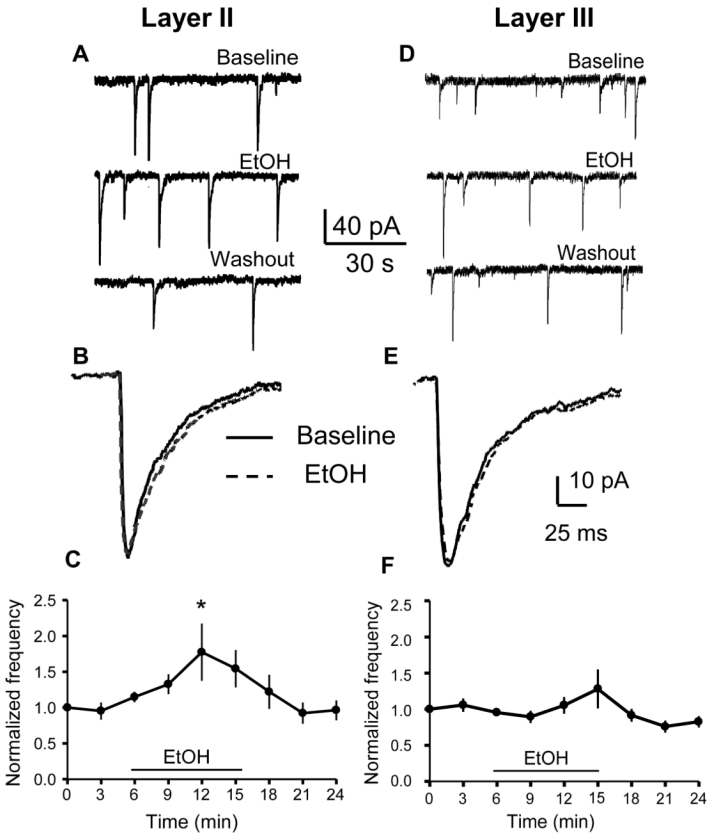

Figure 2. Effect of EtOH on $GABA_A$-sPSC frequency in layer II and layer III pyramidal neurons

(A, D) Sample $GABA_A$-sPSC traces obtained before, during, and after washout of 70 mM EtOH. (B, E) Average $GABA_A$-sPSC traces obtained before (solid line) and after 70 mM EtOH application (dashed line). (C, F) Timecourse of EtOH's effect on $GABA_A$-sPSC frequency (* $p < 0.05$, one-way ANOVA followed by Dunnett *post-hoc* test vs. the 3 min time point; n=8 cells). Data were normalized with respect to an average of responses obtained in the first 3 min of recording.

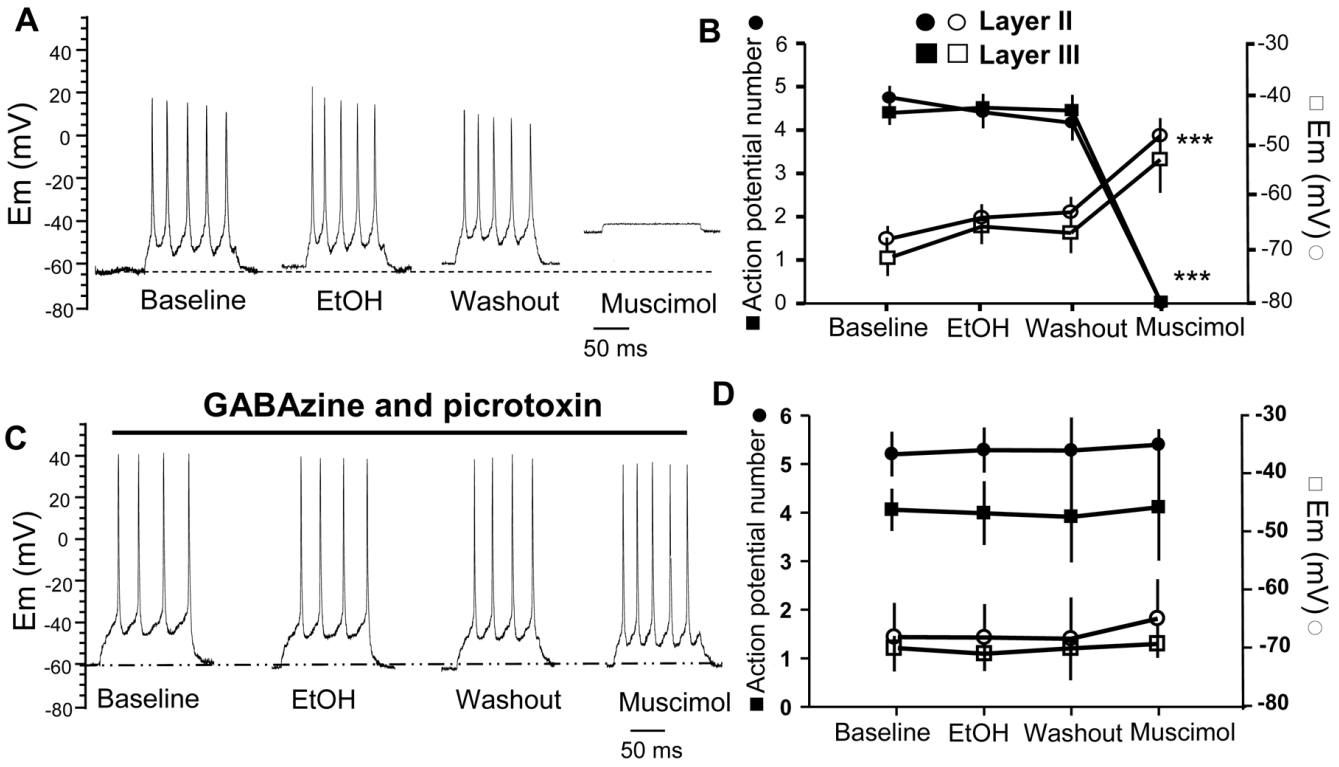

Figure 3. Effect of EtOH on action potential number and E_m in layer II and layer III pyramidal neurons

(A) Representative current-clamp traces obtained in the perforated-patch configuration illustrating responses to injection of 50 pA for 100 ms in layer II. (B) Summary of action potential number and estimated E_m for the indicated experimental conditions. Layer II: action potential (filled circle), E_m (open circle), n=8 cells; layer III: action potential (filled square), E_m (open square), n=7. *** $p< 0.001$ by one-way ANOVA followed by Tukey's *post-hoc* test. (C–D) Same as in A and B but in the presence of picrotoxin (50 μM) and gabazine (10 μM) (n=3 cells per layer).

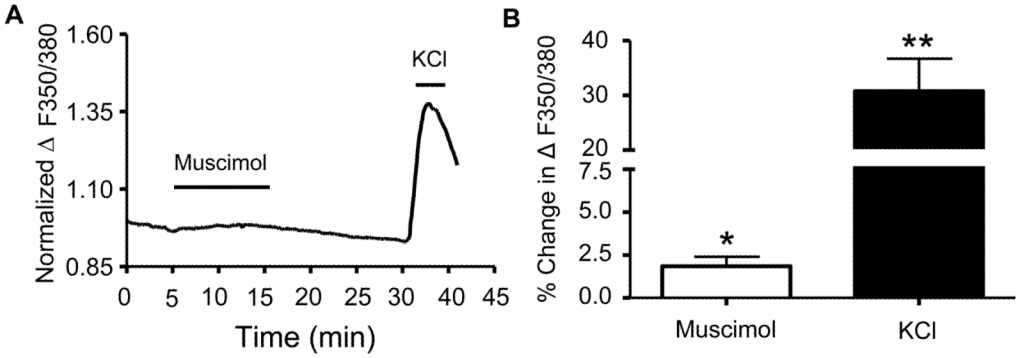

Figure 4. $[Ca^{2+}]_i$ response of layer II/III neurons obtained in presence of ionotropic glutamate receptor antagonists

(A) Average time course for fura-2 $\Delta F/F_0$ response to bath application of muscimol (30 μM) and KCl (40 mM) (n = 5 animals). (B) Average data for conditions shown in A (*p<0.05, **p<0.01 by one-sample t-test; n=5 animals per condition).

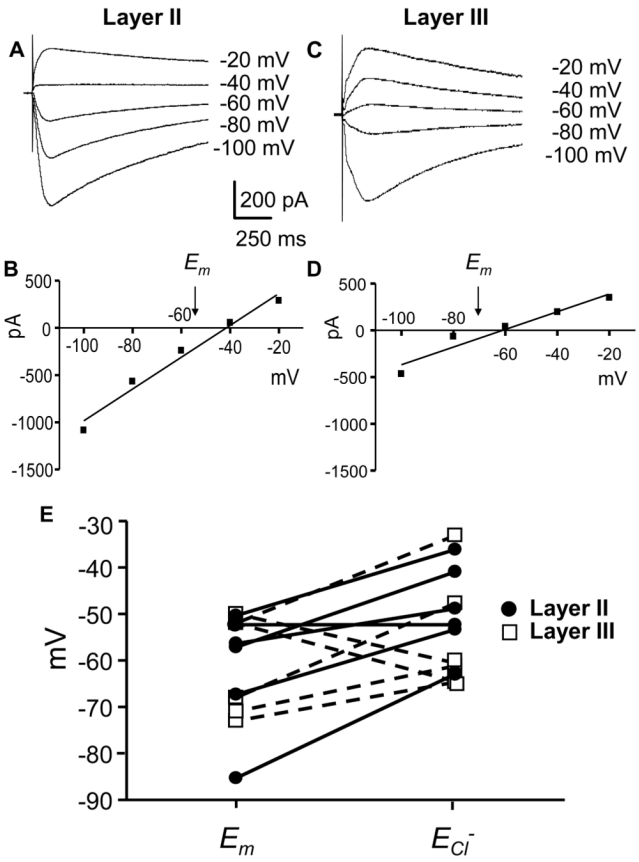

Figure 5. E_{Cl} and E_m in layer II and layer III pyramidal neurons

(A, C) Voltage-clamp traces illustrating currents evoked by pressure application of muscimol (300 μM for 100 ms) at the indicated holding potentials in the gramicidin perforated-patch configuration. (B, D) Peak current-voltage relationships from experiments shown in A and C. Estimated E_m values were determined in the current-clamp mode. (E) Estimated E_m and E_{Cl}^- from 6 layer II (filled circle) and 6 layer III (open square) pyramidal neurons.

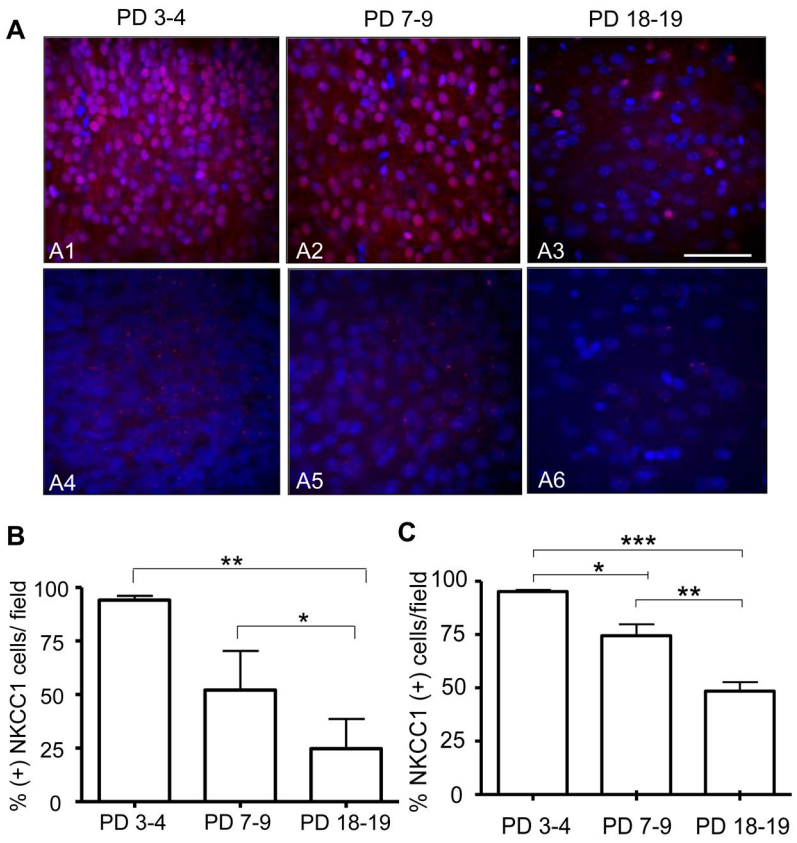

Figure 6. Protein and intranuclear mRNA expression of the NKCC1 co-transporter at three developmental stages in layer II/III of the neocortex

(A1 – A3) 40× confocal images of immunohistochemical experiments performed with an anti-NKCC1 antibody (red) and the nuclear stain, DAPI (blue) (Scale bar 10 μm). (A4–A6) 40× confocal images of FISH assays that were performed with a NKCC1 specific mRNA riboprobe (red) and the nuclear stain, DAPI (blue) (B) Percent of cells that were positive for NKCC1 protein per field as a function of developmental stage (n= 6 animals per age group, ** $p< 0.01$, * $p< 0.05$ by repeated measures one-way ANOVA followed by Tukeys *post-hoc* test). (C) Percent of cells that were positive for NKCC1 mRNA foci per field as a function of developmental stage (n= 6 animals per age group, *** $p< 0.001$, ** $p< 0.01$, * $p< 0.05$ by repeated measures one-way ANOVA followed by Tukeys *post-hoc* test).

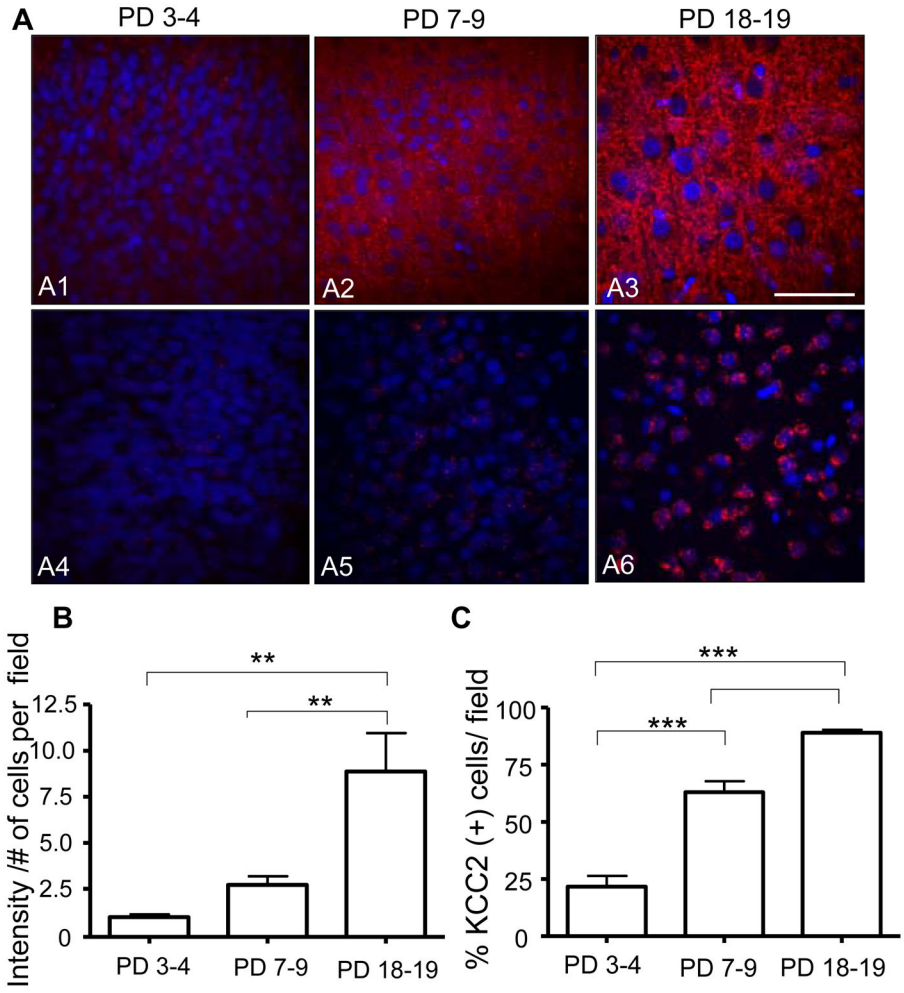

Figure 7. Protein and intranuclear mRNA expression of the KCC2 co-transporter at three developmental stages in layer II/III of the neocortex

(A1 – A3) 40× confocal images of immunohistochemical experiments performed with an anti-KCC2 antibody (red) and the nuclear stain, DAPI (blue) (Scale bar 10 μm). (A4–A6) 40× confocal images of FISH assays that were performed with a KCC2 specific mRNA riboprobe (red) and the nuclear stain, DAPI (blue) (B) KCC2 protein fluorescence intensity (arbitrary units) divided by the number of cell per field as a function of developmental stage (n= 6 animals per age group, ** $p< 0.01$ by repeated measures one-way ANOVA followed by Tukey's *post-hoc* test). (C) Percent of cells that were positive for KCC2 mRNA foci per field as a function of developmental stage (n= 6 animals per age group, *** $p< 0.001$ by repeated measures one-way ANOVA followed by Tukey's *post-hoc* test.

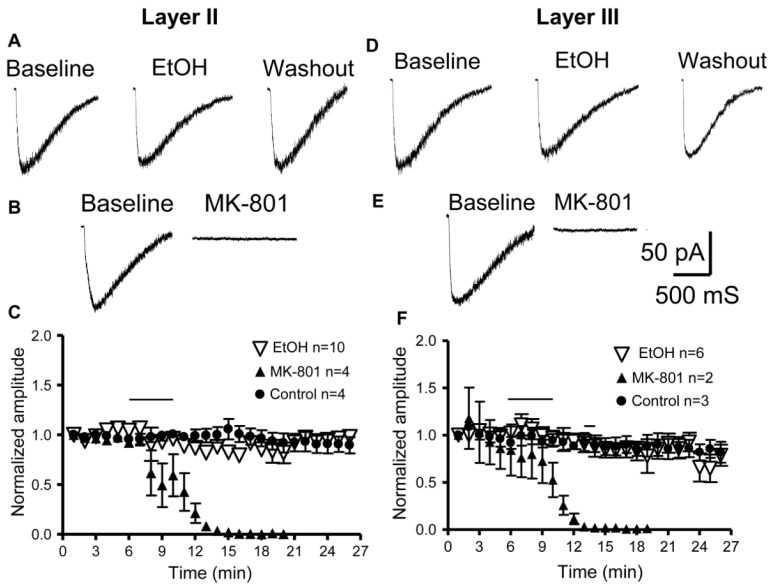

Figure 8. Effect of acute EtOH application on currents evoked by pressure application of NMDA (500 μM) in layer II and layer III pyramidal neurons

Recordings were obtained in the whole-cell voltage-clamp mode at −20 mV. (A, B) Representative currents produced by exogenous application of NMDA in layer II pyramidal neurons in the absence and presence of EtOH (70 mM) or MK-801 (10 μM). (C) Timecourse of NMDA currents obtained from layer II pyramidal neurons under control conditions and in the presence of EtOH or MK-801 (application represented by the horizontal line). (D–F) Same as above but for layer III pyramidal neurons. The error bars are smaller than the symbols in some cases. Data were normalized with respect to an average of responses obtained in the first 3 min of recording.

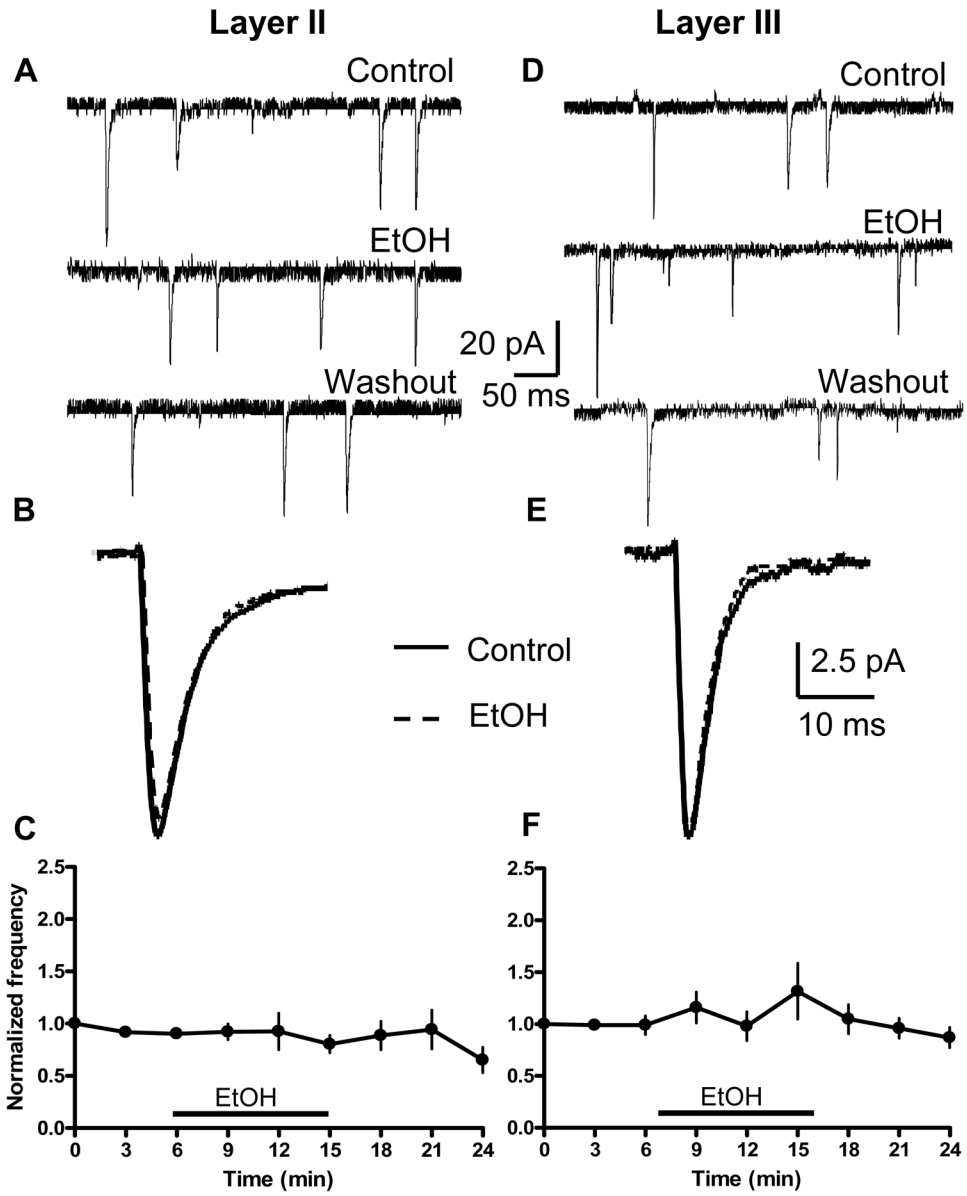

Figure 9. Acute effect of EtOH on AMPA-sPSCs in layer II (left) and layer III (right) pyramidal neurons

(A, D) Sample traces obtained before, during, and after washout of 70 mM EtOH. (B, E) Average AMPA-sPSC traces obtained before (solid line) and after 70 mM EtOH application (dashed line). (C) Timecourse of EtOH's effect on AMPA-sPSC frequency for layer II neurons (n=11 cells). (F) Same as in C but for layer III neurons (n=11 cells). Data were normalized with respect to an average of responses obtained in the first 1–3 min.

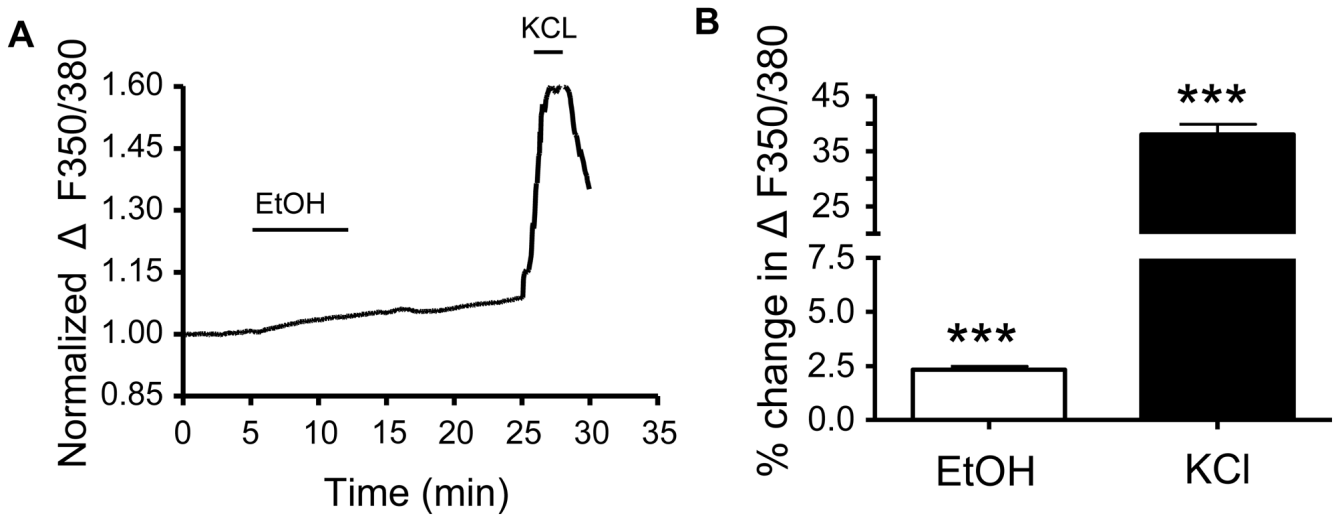

Figure 10. $[Ca^{2+}]_i$ response of layer II/III neurons in the absence of antagonists of neurotransmitter receptors

(A) Average timecourse for fura-2 $\Delta F/F_0$ response to EtOH (70 mM) and KCl (40 mM) (n=5 animals). (B) Average data for conditions shown in A (n=5 animals per brain region; *** $p<0.001$, by one-sample t-test).

Table 1

Electrophysiological Properties of Neocortical Pyramidal Neurons from P7–9 rats[a].

	Layer II	Layer III	b_P
Capacitance	42.66 ± 3.25 pF(n=29)	55.03 ± 3.64 pF (n=24)	0.01
Input Resistance	561.6 ± 46.26 MΩ (n=29)	482.2 ± 49.99 MΩ (n=24)	0.24
Action Potential			
Amplitude	68.93 ± 5.17 mV (n=7)	69.67 ±10.15 mV (n=7)	0.94
Rise time	6.92 ± 0.22 ms (n=7)	5.73 ± 0.44 ms (n=7)	0.03
Spike half-width	1.59 ± 0.18 ms (n=8)	1.75 ± 0.40 ms (n=7)	0.71
GABA-sPSC			
Frequency	0.46 ± 0.09 Hz (n=8)	0.64 ± 0.13 Hz (n=8)	0.31
Amplitude	42.57 ± 4.49 pA (n=8)	48.03 ± 4.47 pA (n=8)	0.41
Half-width	9.88 ± 0.67 ms (n=8)	8.62 ± 0.24 ms (n=8)	0.10
AMPA-sPSC			
Frequency	0.63 ± 0.15 Hz (n=11)	0.76 ± 0.16 Hz (n=11)	0.50
Amplitude	28.64 ± 2.134 pA (n=11)	29.72 ± 3.73 pA (n=11)	0.80
Half-width	3.85 ± 0.26 ms (n=11)	3.45 ± 0.2 ms (n=11)	0.23

[a] All data is from whole-cell patch-clamp experiments, except for action potential data, which was obtained in the perforated patch configuration.

[b] Determined by unpaired t-test.